Geochemistry, Geophysics, Geosystems®

RESEARCH ARTICLE
10.1029/2022GC010377

Special Section:
Africa plate geosystems

Seismogenic Fault Reactivation in Western Central Africa: Insights From Regional Stress Analysis

Hardy Medry Dieu-Veill Nkodia[1], Timothée Miyouna[1], Folarin Kolawole[2], Florent Boudzoumou[1,3], Alan Patrick Rodeck Loemba[1], Nicy Carmel Bazebizonza Tchiguina[1], and Damien Delvaux[4]

[1]Faculty of Sciences and Technics, Department of Geology, Marien NGOUABI University, Brazzaville, Republic of Congo, [2]Lamont-Doherty Earth Observatory, Columbia University, New York, NY, USA, [3]National Research Institute in Exact and Natural Sciences of Brazzaville, Brazzaville, Republic of Congo, [4]Department of Geology, Royal Museum for Central Africa, Tervuren, Belgium

Abstract The onshore continental margins of western Central Africa have been hosting potentially damaging earthquake events for decades; yet, the links between the seismicity, the contemporary stress field, and pre-existing faults are not well understood. Here, we analyze the regional stress fields offshore and onshore along the coastal margin, and in the interior continental areas using earthquake focal mechanisms, map and characterize the detailed structure of preexisting fault systems in outcrops, and assess their reactivation potential. Our results show a switch from NNE-SSW transpressive stress regime offshore and near the coastal margins, to NE-SW compressive and transtensive stress regimes in the cratonic interior (Congo Basin and Kasai Block). We show that regional stresses acting on offshore oceanic fracture zones are compatible with those acting along the onshore areas of the continental margin. Field observations reveal the presence of large fault systems that deform both the Precambrian basement and Phanerozoic sedimentary sequences, with widespread calcite veining, quartz veining, and palygorskite mineralization (with evidence of post-veining shear reactivation) along the fault zones. Along the margin, the preexisting NNE-, NNW-, and N-S -trending strike-slip faults and normal faults show a high slip tendency (>80%–100%), whereas in the continental interior, the NW- and N-S -trending thrust faults are the most likely to reactivate. We argue that favorable orientation of the preexisting faults define the susceptibility of the faults to seismic reactivation. We propose that zones of higher stress magnitudes along distal offshore oceanic fracture zones extend further into the continent and may be driving stress loading on pre-stressed, favorably oriented fault systems onshore, along the continental margin.

Plain Language Summary We investigated the stresses that are generating earthquakes and the compatibility with preexisting fault systems along the supposedly "stable" continental margin of western Central Africa. The stresses acting on the continent interior were also determined and distinguished. Our results show that the stress regimes switch from transpressive offshore and along the continental margin, to purely compressive and transtensive in the continental interiors. Also, we found that the regional stresses acting on offshore oceanic fracture zones are compatible with those acting along the onshore coastal areas of the continental margin. In this stress field, the potential for reactivation of the observable preexisting onshore fault systems is very high, particularly for those oriented NNE-SSW and N-S. We propose that the large stress magnitudes along oceanic fracture zones may extend further into continental areas, leading to earthquakes on the preexisting faults.

Key Points:

- Stress regimes in western Central Africa switch from transpressive near the coastal margin, to compressive and transtensive in the continent
- Regional stresses acting on offshore oceanic fracture zones are compatible with those acting along the onshore continental margin
- Favorable orientation of some pre-existing onshore faults make them susceptible for reactivation

Supporting Information:

Supporting Information may be found in the online version of this article.

Correspondence to:

H. M. D.-V. Nkodia,
nkodiahardy@gmail.com

Citation:

Nkodia, H. M. D.-V., Miyouna, T., Kolawole, F., Boudzoumou, F., Loemba, A. P. R., Bazebizonza Tchiguina, N. C., & Delvaux, D. (2022). Seismogenic fault reactivation in western Central Africa: Insights from regional stress analysis. *Geochemistry, Geophysics, Geosystems*, *23*, e2022GC010377. https://doi.org/10.1029/2022GC010377

Received 8 FEB 2022
Accepted 21 SEP 2022
Corrected 21 NOV 2022

This article was corrected on 21 NOV 2022. See the end of the full text for details.

Author Contributions:

Conceptualization: Hardy Medry Dieu-Veill Nkodia, Timothée Miyouna, Folarin Kolawole, Florent Boudzoumou, Damien Delvaux

1. Introduction

Earthquakes remain one of the most catastrophic natural hazards in human history. Beyond the associated fatalities, earthquakes also leave behind lasting environmental and economic crises in the affected communities. Although, the largest magnitude earthquakes have been recorded along plate boundaries in association with plate subduction, collision, and continental rifting (McCaffrey, 2008), several large magnitude (Mw > 6) events have also been recorded in intraplate regions (e.g.,Talwani, 2014; Tuttle et al., 2002), and more intriguingly, along passive continental rift margins where the sources and occurrence of earthquakes remain less understood. Among the large magnitude and devastating earthquakes recorded in continental intraplate regions previously thought to be relatively stable include the Mw 6.2 Latur Earthquake of 29 September 1993 in South India which

Data curation: Hardy Medry Dieu-Veill Nkodia, Damien Delvaux
Formal analysis: Hardy Medry Dieu-Veill Nkodia
Funding acquisition: Hardy Medry Dieu-Veill Nkodia, Florent Boudzoumou, Damien Delvaux
Investigation: Hardy Medry Dieu-Veill Nkodia, Timothée Miyouna, Florent Boudzoumou, Alan Patrick Rodeck Loemba, Nicy Carmel Bazebizonza Tchiguina, Damien Delvaux
Methodology: Hardy Medry Dieu-Veill Nkodia, Timothée Miyouna, Folarin Kolawole, Damien Delvaux
Project Administration: Hardy Medry Dieu-Veill Nkodia, Florent Boudzoumou, Damien Delvaux
Resources: Hardy Medry Dieu-Veill Nkodia, Damien Delvaux
Supervision: Hardy Medry Dieu-Veill Nkodia, Florent Boudzoumou, Damien Delvaux
Validation: Hardy Medry Dieu-Veill Nkodia, Folarin Kolawole, Damien Delvaux
Visualization: Hardy Medry Dieu-Veill Nkodia, Folarin Kolawole
Writing – original draft: Hardy Medry Dieu-Veill Nkodia
Writing – review & editing: Hardy Medry Dieu-Veill Nkodia, Timothée Miyouna, Folarin Kolawole, Alan Patrick Rodeck Loemba, Nicy Carmel Bazebizonza Tchiguina, Damien Delvaux

claimed a death toll of 11,000 (Gupta et al., 1998) and the Mw 6.2 Guinea earthquake of 22 December 1983 which caused 1,500 fatalities and significant property damage (Musson, 1992; Suleiman et al., 1993). On the causes of intraplate seismicity, proposed hypotheses include stress buildup (e.g., Calais et al., 2016; Kolawole et al., 2017, 2019; Ngatchou et al., 2018; Schulte & Mooney, 2005; Stein et al., 1989; Sykes, 1978; Zoback & Richardson, 1996) driven by far-field stress transmission from active plate boundaries (Delvaux & Barth, 2010; Delvaux et al., 2016; Nkodia et al., 2020; Wiens & Stein, 1983, 1985), gravitational body forces (Levandowski et al., 2017), deglaciation-related isostatic rebound (Lund Snee & Zoback, 2020), underground industrial activities (Grigoli et al., 2017; Keranen & Weingarten, 2018), and thermal weakening of the lithosphere (Holford et al., 2011).

Some passive rifted margins across the world are known to host pronounced distributed seismicity, among which are well-instrumented regions such as the eastern Brazilian Atlantic margin (Assumpção, 1998), the southern Australian margin (Holford et al., 2011), and the eastern North American margin (Sbar & Sykes, 1973; Zoback, 1992). However, in poorly instrumented regions, such as Equatorial West Africa and western Central Africa where knowledge of the seismicity is scarce, the relation between the acting present-day stress regime, the sources of stress perturbation, and the mechanics of reactivation of inherited structures are still poorly known (Olugboji et al., 2021). This knowledge gap hinders the development of viable early warning mechanisms for hazard mitigations in local communities located in such regions and therefore justify a special attention.

In this study, we explore the passive margin of western Central Africa, an area which shows significant intraplate seismicity in both its offshore domains and within the continent (Figures 2a and 2b). This region has been the subject of much research for almost a century (Ambraseys & Adams, 1986; Amponsah et al., 2012; Delvaux & Barth, 2010; Heidbach et al., 2018; Junner & Bates, 1941; Kadiri & Kijko, 2021; Krenkel, 1923; Musson, 1992; Nwankwoala & Orji, 2018; Oladejo et al., 2020). Although most of the studies focused on the use of remote sensing to provide a seismotectonic model for the region (Adepelumi et al., 2008; Awoyemi & Onyedim, 2004; Awoyemi et al., 2017; Bouka Biona & Sounga, 2001; Oladejo et al., 2020), the characterization of the structures is sparse, and there remains a limited understanding of the detailed structure and current stress state of the potentially seismogenic preexisting faults.

The aim of this contribution is to evaluate the possible current regional stress regime that is most dominant and its ability to reactivate the preexisting fault structures along the western Central African passive margin by using the slip tendency analytical techniques. By determining which types of structures that are being reactivated within the study area and the associated kinematics, we intend to new insights into the seismic hazards and possible drivers of seismicity along the margin. We anticipate that our results will contribute to a better assessment of the seismic hazard and the associated coseismic ground motions for this region.

2. Geological and Tectonic Setting

2.1. Regional Geology of Western Africa and Continental Margin

The Western - Central Africa continental region is mainly dominated by Archean to Mesoproterozoic cratonic basement, overlain by Neoproterozoic and Phanerozoic units (Figure 1). The cratonic basement rocks outcrop within the Congo Craton in Central Africa region and in the West African Craton northwest of our study region. These cratons are formed by Archean blocks limited by Proterozoic terranes and shear zones, and host large sedimentary basins such as the Neoproterozoic-Phanerozoic Taoudeni and Congo sedimentary basins (Figure 1). The Congo Craton consists in an assemblage of five Archean nuclei welded together by Paleo- and Mesoproterozoic belts (De Wit & Linol, 2015; Thiéblemont et al., 2009; Turnbull et al., 2021): (a) the Ntem-Chaillu block in the central and northwestern domains, covering the region of Cameroon, Gabon, and Republic of Congo (RC) (Kessi, 1992; Tchameni et al., 2000); (b) the 2.5 Ga Angola block to the south in Angola (De Carvalho et al., 2000; Jelsma et al., 2018); (c) the 3.6–2.5 Ga Kasaï block to the southeast in Democratic Republic of Congo (DRC) (Batumike et al., 2006); (d) the 3.2–2.5 Ga NE-Congo Block in the Northern DRC (Turnbull et al., 2021), and (e) the 2.8–2.6 Ga Tanzanian block.

These cratonic blocks have underwent multiple episodes of large-scale brittle deformation which created large discontinuities within them. Akame et al. (2020, 2021) documented the presence of large NW-SE, NE-SW and E-W trending brittle and ductile shear zones in the Ntem-Chaillu block, inherited from Neoarchean orogenesis. Similar deformation were also reported in the laterally equivalent Souanké Archean rocks in the Ivindo region

of Republic of Congo (Gatsé Ebotehouna et al., 2021; Loemba et al., 2022). In the Souanké domain, the brittle shear zones show evidence of reactivation into normal faulting kinematics interpreted to be related to the Cretaceous opening of Atlantic Ocean (Gatsé Ebotehouna et al., 2021; Loemba et al., 2022).The Ntem-Chaillu block is bounded to the north by the Oubanguides Belt which developed during the Pan-African Orogeny (550 ± 100 Ma) and was subsequently deformed in the Mesozoic by the continental-scale, NE-trending Central African Shear Zone (CASZ; Figure 1). The CASZ, which extends into the Borborema province of NE Brazil (Miranda et al., 2020), is considered to be an accommodation zone that was activated during the opening of the South Atlantic (Moulin et al., 2010; Ngako et al., 1991, 2003; Njonfang et al., 2008; Wilson, 1965). Recent earthquakes and associated source mechanisms along a segment of the CASZ (e.g., 2005 Montalé, Cameroon earthquake) suggests that the CASZ structure may still be active as the Atlantic Ocean basin continues to open (Ngatchou et al., 2018).

Along the western margin of the Congo Craton, the Ntem-Chaillu and Angola cratonic blocks are separated by the Pan-African West-Congo Belt (630–490 Ma) the western part of which was later rifted during the opening of the Atlantic Ocean (Alvarez & Maurin, 1991; Boudzoumou & Trompette, 1988; Bouenitela, 2019; Fullgraf et al., 2015; Hossié, 1980). The fold-and-thrust terranes of the West-Congo Belt host large (>90 km-long) NE-SW, NW-SW and N-S trending brittle shear zones (Alvarez & Maurin, 1991; Nkodia et al., 2021). In RC, DRC, and Angola, the terranes of the mobile belt are covered by early Paleozoic sandstones which record two main phases of strike-slip deformation, first during the Gondwanide Orogeny in the Permo-Triassic, then during Cretaceous opening of the Atlantic (Miyouna et al., 2018; Nkodia et al., 2020). The early Paleozoic sandstones of the Inkisi Group show reactivated and segmented strike-slip fault zones oriented NW-SE, NE-SW, and E-W, observable in outcrops (Miyouna et al., 2018; Nkodia et al., 2020) and in seismic reflection images (Delvaux et al., 2021; Kadima et al., 2011).

The phases of Late Paleozoic-Early Mesozoic contractional tectonic deformation in the Congo Basin are observable across eastern and southern Africa (Delvaux et al., 2021). However, there is evidence for the presence of through-going structures which deform both the Paleozoic-Mesozoic and Cenozoic sedimentary sequences (Delvaux et al., 2021; Kadima et al., 2011), suggesting there might still be on-going intra-continental tectonic deformation in Central Africa. Mbéri Kongo (2018) showed that the Cretaceous sandstones deposits of the Bateké Plateau on the margin of the Congo Basin have been deformed by large strike-slip faults with associated conjugate normal faults. Northwest of the Oubanguides Belt, in West Africa, the Cretaceous intracratonic Benue Rift developed within the Trans-Sahara Mobile Belt as a corridor of transtensive faults with associated magmatism (Ajakaiye et al., 1986; Benkhelil, 1989; Oha et al., 2020). The closure and abortion of the rift occurred in the Santonian, associated with a transpressional deformation of its Cretaceous syn-rift deposits (Benkhelil, 1989; Ofoegbu, 1985). The Trans-Sahara Mobile Belt host several N- to NNE-trending shear zones associated with the Proterozoic amalgamation of West Gondwana. Some of the shear zones also record evidence of brittle deformation during the opening of the Atlantic Ocean, an example of which is the Kandi fault zone which served as an accommodation zone during the rifting event (Affaton et al., 1991).

2.2. Oceanic Fracture Zones in the Gulf of Guinea, Western Nubian Plate

The oceanic crust of the Atlantic Basin dominates the western portion of the Nubian Plate and hosts several fracture zones that extend eastward from the active transform faults at the Mid-Atlantic Ridge plate boundary toward western Africa's rifted continental margin (Figure 1). Oceanic transform faults developed within the oceanic crust starting sometime after continental break-up and serve to accommodate the lateral movement of tectonic plates, and lateral variation of spreading rates, and to facilitate connectivity between ridges and trenches (De Long et al., 1977; Gerya, 2012; Hensen et al., 2019). Due to their strong topographic expression at the sea floor, their structural and geochemical alteration of the oceanic crust, and temporal accretion patterns, transform faults and oceanic fracture zones are mappable in bathymetric, seismic reflection, gravity, and magnetic data sets (Delteil et al., 1974; Fail et al., 1970; Gorini & Bryan, 1976; Guiraud et al., 2010; Mascle & Sibuet, 1974).

Although the active plate boundaries (i.e., spreading oceanic ridges and subduction zones) host most of the seismicity of oceanic basins, oceanic fracture zones and their flanking areas also accommodate significant seismic activity and represent seismic hazards within intraplate areas away from the plate boundaries (Figure 2a; Burke, 1969; Lay, 2019; Okal & Stewart, 1982). On the lateral growth of oceanic fracture zones,

Figure 1. Map of the bedrock geology of (a) the Nubian Plate and (b) the western Central Africa sub-region, showing major litho-tectonic subdivisions of the crust and previously mapped fault systems. WCFS1, WCFS2, IFS, and SFS, represent field sites where structural measurements of fault systems were collected. WCFS1 represent the western domain of the West Congo Fault System primarily dominated by thrust faults, whereas. WCFS2 is the eastern domain dominated by strike-slip faults. IFS represents the field study sites of fault systems in the Inkisi Group in Brazzaville and Kinshasa areas. SFS represent fault system collected in Souanké region. AFZ, Akwapim Fault Zone; BFZ, Boundary Fault Zone; CASZ, Central African shear zone.

Figure 2. Regional earthquake distribution and focal mechanism solutions. (a) Map of the distribution of earthquakes in the Western African passive margin. AFZ, CASZ are the Akwapim Fault zone, the Central Africa shear zone. (b) Map of distribution of focal mechanism obtained from published literature (e.g., Delvaux & Barth, 2010; Meghraoui et al., 2016; Suleiman et al., 1993), Global CMT moment tensor, and GFZ GEOFON earthquake catalogs.

Burke (1969) proposed a mechanism of propagation toward the continents by extension fracture mode which produce stress transmission that initiate seismic failure at the continental margins. Also, Fairhead et al. (2013), mentioned a possible link of transforms with Central African rift development—although it is not present day tectonics, it is a link between older crustal deformation onshore and transform activity offshore.

In the Atlantic Ocean, some of the most active fracture zones which commonly extend close to- or into the western Africa rifted continental margin include the Romanche, Chain, Charcot, Ascension, and Saint Paul fracture zones (Figures 2a and 2b; Heezen et al., 1964, 1965; Mascle & Sibuet, 1974). A few studies argue for the lateral continuation of the oceanic fracture zones onto the continent of West Africa and causative relationship with onshore earthquakes. This is based on the alignment of on-shore magnetic lineaments in Nigeria with the trends of the offshore fracture zones (Ajakaiye et al., 1986), on the colocation and alignment of rifted transform margins such as the Ghanaian and Ivorian coastline with the Romanche and St Paul fracture zones respectively (Figure 2a; Antobreh et al., 2009), and on the recent (<10 million years) acceleration of strain rates on oceanic transform faults post-continental break-up in the Late Cretaceous (Meghraoui et al., 2019). However, questions remain on the link between the current stress regime acting on the margin of western African continent and the mechanisms and triggers of seismic reactivation of preexisting structures.

3. Data and Methods

3.1. Earthquake Data and Stress Indicators

For the study region (between latitudes 16.70°N and 14.07°S, and longitudes 23°W and 24.66°E), we built a database of earthquakes from publicly accessible global catalogs which includes the International Seismic Center (ISC), the United States Geological Survey (USGS), the Global Centroid-Moment-Tensor (CMT), and the GFZ GEOFON earthquake catalogs (displayed on Figure 2a).

The focal mechanism solution data base (See Table S1 in Supporting Information S1) was initially compiled from literature, Global CMT moment tensor, and GFZ GEOFON earthquake catalogs for the paper of Delvaux and Barth (2010). It was further updated and completed by one of us (D. Delvaux) for the seismotectonic map of Africa (Meghraoui et al., 2016). In cases where the focal mechanism solution of the same earthquake event is recorded by multiple earthquake databases, we considered the most recent one in order to guarantee the precision of the resulting stress tensor solutions (Ayele, 2002; Barth et al., 2007; Craig et al., 2011; Suleiman et al., 1993). Relative to the compilation for the seismotectonic map of Africa, only one new focal mechanism (from Ngatchou et al., 2018) has been added. They are displayed as beachballs in Figure 2b and color-coded stress regime in Figure 3 and SHmax orientations. In addition to the focal mechanisms of earthquakes, we compiled also some borehole breakouts as additional stress indicators (not used in the stress inversion) from the Worl Map stress data base (Heidbach et al., 2018).

3.2. Mapping of Tectonic Lineaments

In order to delineate mega-scale tectonic structures in the oceanic crust and around the onshore continental coastal margin, we utilized hillshaded Digital Elevation Model (DEM) maps generated from bathymetric and topographic data. In the offshore areas, we delineated and mapped the traces of oceanic fracture zones on DEM of bathymetric data extracted from GEBCO (GEBCO Bathymetric Compilation Group 2021, 2021), which has a spatial resolution of 1 arc min (~1.5 km). Within the onshore continental areas, using previously published geologic maps and field observation where possible (see details in Section 3.3) as constraints, we manually interpreted and digitized visible structural lineaments defined by steep laterally continuous topographic relief gradients from a mosaic of scenes of a 30 m resolution ALOS-type radar interferometric digital elevation model (DEM) images, following a standard approach (Burbank & Anderson, 2011). The ALOS data was obtained from the ALOS Global Digital Surface Model (https://www.eorc.jaxa.jp/ALOS/en/aw3d30/data/index.htm). The previously published geologic map that guided the lineament interpretation is the tectonic map of Africa by Milesi et al. (2010) in which the faults were compiled from field studies and gravity anomalies, conducted by geological surveys groups of different countries.

3.3. Field Observations and Collection of Structural Measurements

Onshore, along the continental margin of western Central Africa, recorded seismicity occurs in the northern parts of the West Congo Belt and surrounding basement terranes (Figures 2a and 2b). However, due to limited access to this region at the time of this study, we perform our field study in the southern extension of the West Congo Belt and the associated fault systems in the onshore areas of RC and DRC. The field campaigns were conducted in the regions of Brazzaville, Dolisie, and Souanké regions of RC, and in the Kongo Central (ex-Bas-Congo) region of DRC. The field locations are located along the West Congo Fault System (WCFS1 (western part) and WCFS2 (eastern part), Inkisi Fault System (IFS), and Souanké Fault System (SFS) (see Figure 3a). We conducted field observations and collection of structural data along the fault and fracture systems in outcrops. The field campaign served as ground-truthing to constrain the mapping of structural lineaments in hillshaded maps; and to confirm the geologic origin of some of the interpreted lineaments as fault strands or brittle shear zones where they are accessible. In the field outcrops of the faults and brittle shear zones, we collected measurements of strike and dip of fault planes, trend and plunge of slip vectors (striations) along the surfaces, and we documented evidence and characteristics of geochemical alterations of the fault zones. We have provided information on our field measurements in Tables S2–S6 of this manuscript. The structural field measurements provide fault plane orientation data that we used as one of the inputs into the slip tendency analysis (see Section 3.4).

3.4. Assessment of Contemporary Stress Field From Earthquake Focal Mechanisms

The contemporary stress field from the inversion of focal mechanisms has been assessed in a similar way as in Delvaux and Barth (2010), using the methodology of Delvaux and Sperner (2003). With the Win-Tensor program (Delvaux, 2011, 2012), we determined the current stress field acting on the Gulf of Guinea section of the Nubian Plate, using the information on source parameters of earthquake focal mechanism solutions as input data. For our analysis, we considered that the available focal mechanism solutions are sparse and the seismicity is distributed across offshore and onshore areas along the coastal rifted margin and in the cratonic interior. We divided the study region into three sub-regions defined by as three boxes (Boxes 1–3, Figures 2 and 3), by assuming that each box has a uniform stress field. Box 1 covers the Gulf of Guinea and the coastal margin of Ivory Coast, Ghana, Nigeria and Gabon (Figures 3a and 3b), Box 2 covers the continental interior (Gabon-Cameroon-Congo continental margin and western part of the Congo Basin) (Figures 3a and 3c) and Box 3 covers the SW margin of the Congo Basin Kasai region in the DRC and Angola (Figures 3a and 3d).

The Win-Tensor program uses the stress inversion method (Angelier, 1975, 1989; Angelier & Mechler, 1977) to determine a reduced tensor which contains the orientations of the principal compressive stress axes ($\sigma1$, $\sigma2$, and $\sigma3$) and the stress ratio R $(\sigma2-\sigma3)/(\sigma1-\sigma3)$ which expresses the relative stress magnitudes. The program first estimates the tensor solution using the PBT (compression, intermediate and tensional) axes method and the Right Dihedron method. This initial stress tensor solution serves as a starting point to determine a more constrained tensor solution using an iterative Rotational Optimization method. In the latter, it uses only the focal planes as stress indicator and tries to adjust the stress tensor that best explain the slip on these planes by an iterative procedure. We used the misfit function F5 in the Tensor program (described as F3 in Delvaux and Sperner [2003]), that minimizes the difference between the calculated slip direction and the resolved direction (α) and favor slip on the plane by maximizing the resolved shear stress magnitude and minimizing the normal stress magnitude.

As we cannot access to the absolute magnitudes with focal mechanism data only, we use dimensionless magnitudes. This misfit function is independent from the differential stress (expressed by the ratio $\sigma3/\sigma1$), and its values vary from 0 to 360°. As in Delvaux and Barth (2010), we first invert the focal mechanism data using both nodal planes as if they were independent data. Because the number of focal mechanism is rather limited, in a second step, we only removed from the inversion the worst fit auxiliary plane whose values of the misfit function exceeds the arbitrary value of 30. The stress regime index R' typify the regime associated with the solution tensor. R' is computed from the R ratio, taking into account which stress axis is subvertical, and gives the type of stress regime in a continuous scale of 0–3 (Delvaux & Sperner, 2003; Delvaux et al., 1997). The type of stress regime is also illustrated in Frohlich triangular diagrams (Frohlich, 1992). Every tensor obtained is associated to a quality rank parameter range from A to E. (A for very good, B: Good, C: fair, D: poor, E: very poor) as defined in Delvaux and Sperner (2003). In addition, standard deviation for the horizontal stresses (SHmax/Shmin) and the stress ratio R' are computed as in Delvaux (2012).

3.5. Assessment of Slip Tendency of the Preexisting Structures

The slip tendency is a well-established procedure for assessing the reactivation potential of pre-existing fractures and faults under a given stress field (Morris et al., 1996). It is generally used in the seismic hazard assessment where it consists in the application of stress tensors inverted from focal mechanisms on a known fault system in order to compute to evaluate their reactivation potential in the form of the Slip Tendency ratio. Unfortunately, in the present case, the focal mechanism data do not cover the area where we have information on the fault structures in RC and the DRC. Therefore, we will test the stress tensors obtained from the surrounding areas and examine their respective likelihood to reactivate the known fault systems.

Seismicity is caused by sliding on a fault plane which forms a pre-existing weakness plane. According to the Mohr-Coulomb criterion of fault reactivation, frictional sliding on a pre-existing fracture which acts as a plane of weakness occurs when the shear stress σ_s on a plane exceeds the failure shear strength σ_f. It depends from the cohesion C, the friction coefficient $\mu = \tan \varphi$ (with φ the angle of internal friction) and the effective normal stress on the plane σ_n' (Angelier, 1989; Fossen, 2016):

$$\sigma_s \geq \sigma_f = \mathrm{C} + \sigma_n' \tan \varphi = \mathrm{C} + \sigma_n' \mu$$

The slip tendency Ts computed as the ratio of the shear to normal stresses resolved on a fault or fracture surface under a given stress field. Following Morris et al. (1996), the slip tendency Ts on a surface is defined as the ratio of shear stress (σ_s) to normal stress on that surface (σ_n) :

$$\mathrm{Ts} = \sigma_s / \sigma_n$$

The normalized slip tendency T*sN* (values between 0 and 1) is obtained by normalizing the Ts value relative to the maximum possible value max (Ts):

$$\mathrm{TsN} = \mathrm{Ts}/\max(\mathrm{Ts})$$

For reactivating a fault, the ratio of σ_s/σ_n (and thus Ts) must lie above the lines of initial friction defined by its coefficient of friction $\mu = \tan \varphi$, with $\tan \varphi = \sigma_s/\sigma_n$ (Angelier, 1989; Fossen, 2016). On the Hoover Dam test case, Angelier (1989) obtained minimum coefficient of friction for fault reactivation of 0.3 for normal faults and 0.5 for strike-slip faults (corresponding slope angles of 17° and 27°). On the fractures analyzed in the Pool area, we obtained slope angles of 30° (friction coefficient of 0.57) for the inversion of the different strike-slip fault systems (Delvaux et al., 2017 and work in progress).

In the present case, where we have a strike-slip stress regime, we consider that the planes with a slip tendency above 0.6 are likely to be reactivated under the tested stress tensor. We used the ratio between the extreme stress magnitudes σ_3/σ_1 of 0.05 which implies de-facto a certain cohesion (see Mohr diagrams in Figure 7). We note also that slip tendency is always determined by assuming the faults surfaces are cohesionless (Morris et al., 1996).

4. Results

4.1. Spatial Distribution of Earthquakes and Mapped Tectonic Lineaments

Offshore, seismic events are either collocated with or occur in the vicinity of traces of oceanic fracture zones which show dominant trends of ENE and NE (Figures 2 and 3). Some events also occur along the Cameroon volcanic line and around the Bié Dome in Angola. Onshore, along the coastal margin and continental interior areas, the regional seismicity patterns show clustering of events that are collocated with or in vicinity of the mapped tectonic lineaments (Figures 2 and 3a). For example, at the location of field site SFS, the epicenter of a Mw 6 event is collocated with the trace of a large ENE-to-NE trending fault system in the Ntem-Chaillu Block (see lineament with label "SFS" in Figures 1 and 3a). In the northern parts of the West Congo Belt and surrounding basement terranes (southern Cameroon and Gabon; Figures 2a and 2b), the earthquake focal mechanisms show NNW-SSE and NW-SE SHmax (maximum horizontal compressive stress) orientations (Figures 3a and 3b) controlling slip on NNE, NNW, NE, NW, and E-W -trending nodal planes (Figure 4a). The frequency-azimuth and length-azimuth distribution of large-scale fault lineaments in these northern areas show orientations that align with the earthquake nodal planes (Figure 4a). In the southern continuation of the West Congo Belt and its fault systems where our field work was carried out (RC and DRC), frequency- and length-azimuth distributions

Figure 3. (a) Regional boxes and SHmax orientations calculated from earthquake focal mechanism solutions in the western part of the Nubia Plate. Zoomed-in view of the different sub-regions in which stress inversion is carried out (i.e., boxes "Boxes 1 to 3" in panel [a]) and the resulting showing stress regimes. Panels (b–d) show respectively Box 1, Box 2, and Box 3 respectively. The pie-chart show the frequency distribution of the different tectonic.

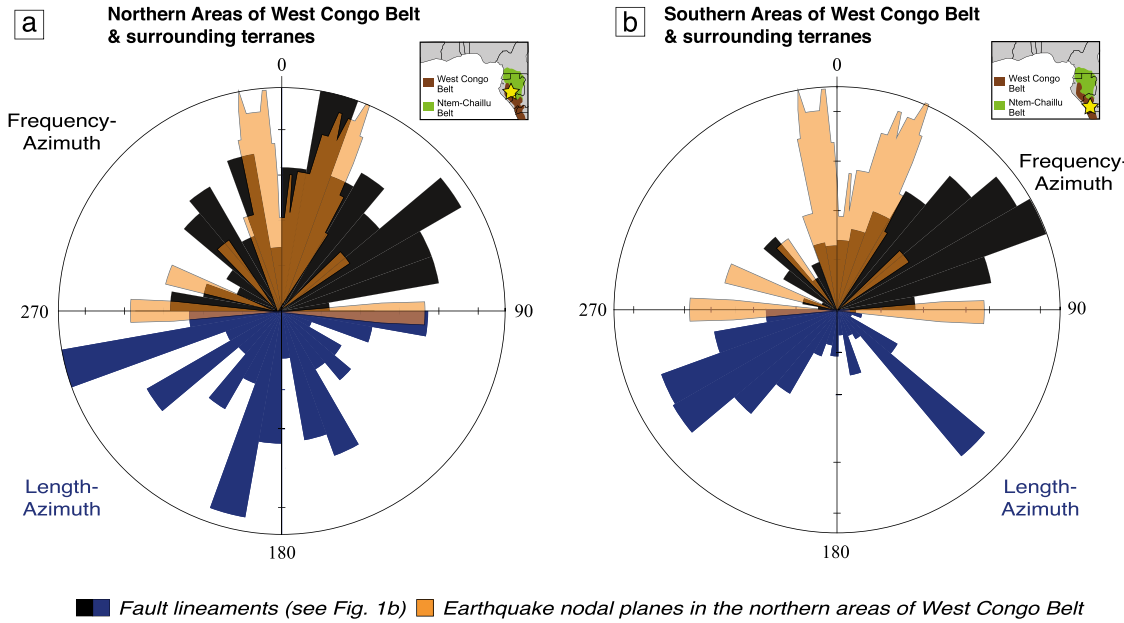

Figure 4. Comparison of earthquake focal mechanism nodal planes with fault lineaments in the (a) northern and (b) southern parts of the West Congo Belt and neighboring terranes (onshore coastal areas of western Central Africa). The plots show that observable fault orientations in the northern areas (where the recorded earthquakes are located) are also well represented in the southern areas (where our field structural measurements were carried out).

of fault lineaments show the occurrence of similar fault trends as those in the northern areas (Figure 4b). This similarity is also valid for the earthquake nodal planes (Figure 4b).

Just offshore along the Ghanian margin, earthquakes cluster at the location where the Romanche Fracture Zone extends close to the Ghana shoreline (Figures 2b and 3a); and at least one of each of the nodal planes on the associated focal mechanism solutions show a trend that is parallel or sub-parallel to the fracture zone orientation (Figure 2b). In southern Ghana and surrounding regions, tectonic lineaments show dominant sets trending NNE and ENE of which the latter is parallel to the trend of the Romanche Fracture Zone (Figures 3a and 3b). In the entire study region, Most of the focal mechanism solutions of the earthquakes show a codominance of thrust fault and strike-slip fault regime (Figure 3). Only 24% of events show normal faulting regime (rose diagrams in Figure 3) and most are restricted to the rifted costal margin. Within the continental interior, the strike-slip and reverse faulting regime appear to be distributed across a broad region which includes also the Congo Basin.

4.2. Fault Structure in the Field Outcrops

In the field, the study area appears dominantly affected by strike-slip faults trending NW-SE, NE-SW, and minor ENE-WSW to E-W. They are of various types and result from the Paleozoic to Cenozoic tectonic evolution. At the field sites in RC and DRC, observable deformation in the Paleozoic sandstones of the Inkisi Group mostly showed steep strike-slip faults and joints. Almost all strike-slip faults are arranged in relay segments or in a corridor of segments connected by extension fractures (Figures 5a and 5d). Some are seen over more than 600 m long in the river bed. The related lineaments mapped in regional-scale DEM hillshaded maps reach up to 80–90 km. In quarries, cross-sectional views of the fault-fracture systems show exposures of up to 50 m in height.

The fold and thrust terrane of the West Congo Belt is composed of two domains with distinct structural styles. One of the domains is dominated by major NW-trending low-to high-angle thrusts which control the NE vergence of the belt, and their associated high-angle back-thrusts (Figure 5b). This structural style primarily affected schistose rocks with intruded dolerite, diamictites, quartzites, and sandstones units. The other domain is more tabular and is dominated by carbonate sequences which are cut by major NE-trending strike-slip brittle shear zones (Figure 5e). The strike-slip shear zones are arranged in step-overs associated with én-echelon extension fractures or normal faults. These faulting styles are well observable down to 100 m depths in the caves of Ngovo and Ndimba. In northern RC, Archean rocks of Souanké host 2.8 Ga charnokites, gneisses, and pegmatites which are also deformed by

Figure 5. Field observations of the intraplate faults systems. (a and d) Fault systems in outcrops of the Inkisi Group (IFS), showing fracture patterns (highlighted in white dashed line in Figure 6a), and a fault zone showing segmented faults in a duplex zone (in Figure 6d), at the Kombé quarry, located near the Congo River, Brazzaville. (b and e) Faults systems (WCFS1 and WCFS2) in the West-Congo Belt showing successively thrust and back-thrust affecting schists and quartzites, in Dolisie along the RN1 primary road, and strike-slip fault planes in Kolas quarry near Loutété region. (c and f) Faults systems (SFS) in Souanké showing high-angle planes of strike-slip faults in the area (in Figure 6c) and, a NE-trending plane that shows horizontal striae that is over-printed by vertical striae associated with calcite fibers, indicating a later normal faulting reactivation of the strike-slip faults. The dashed lines in Figure 6f represent the directions of striae.

the brittle shear zones. Nearly all the brittle shear zones observed on the field show linking architecture with relay zones connected either by extension fractures or duplex structures (Figure 5c). On a slip surface along the strike-slip faults, we find evidence of over-printing of strike-slip slickenlines by dip-slip ones (Figure 5f), indicating that these NE-SW, WNW-ESE, NW-SE and N-S trending strike-slip faults have been reactivated in dip slip.

In addition to the observed brittle deformation along the fault systems, we also note widespread evidence for fluid circulation and precipitation along the fault zones. For example, at field sites WCFS1 and WCFS2 located in the West Congo Belt, several strike-slip fault zones show calcite mineralization that occur in slicken fibers with associated chatter marks steps (Figures 6a–6c), and a few other fault zones show iron staining along the fault planes (Figures 6b–6d). Likewise, in the fault zones hosted in schistose terranes (e.g., WCFS1 and WCFS2), we observe networks of quartz veins injected along thrust faults and shear zones (Figure 6f). In the sedimentary sequences (Inkisi Group; location IFS), the fault zones are either mineralized by palygorskite, calcite, or a mix of both (Figure 6e). However, at all the field sites visited, we commonly observed brittle reactivation of the mineralized fault and fracture planes evidenced by sheared mineral fibers with characteristic chatter marks, or tensile fracturing of the mineralized zones.

4.3. Contemporary Stress Fields Within the Analyzed Sub-Regions (Boxes)

The stress inversion of the focal mechanisms (Table 1, Figure 7) gives a transpressive strike-slip stress regime for box 1 ($R' = 1.85 \pm 0.17$), a compressional regime for Box 2 ($R' = 2.58 \pm 0.44$) and an extensional strike-slip stress regime for box 3 ($R' = 1.04 \pm 0.25$). The maximum horizontal compressive stress (SHmax) orientation is NNE-SSW for box 1 (N12°E ± 7.1), ENE-WSW for Box 2 (N66°E ± 19.6), and E-W for Box 3 (N86°E ± 9.6). The quality of tensor solutions is of B type, indicating that they are well-constrained. The points on the Mohr diagrams generally lie above the friction line corresponding to 20° friction angle, except for two focal planes in Box 2. A large proportion of focal planes have been used (10/14 for Box 1, 14/18 for Box 2 and 10/12 for Box 3) and most of the events have been used, except one in each box.

Figure 6. Mineralized fault surfaces and slip indicators. (a) Calcite slicken fibers and associated chatter marks Accretion calcite steps along NW-SE strike-slip faults in carbonates rocks of the West Congo Belt, DRC. (b and c) Carbonate-hosted faults surfaces covered by sheared calcite mineralization accretion calcite steps and iron staining. Note that the carbonate rock in b has penetrative cross-bedding structures that should not be confused with slickenlines. (d) Fault surface in Inkisi sandstones associated with iron alteration realm. (e) Slicken sided palygorskite along a fault in IFS fault system. (f) Deformed doleritic intrusion along a high-angle thrust fault (230/40) injected with quartz veins in the WCFS faults system.

All boxes show strike-slip nodal planes that are oriented NW-SE and NE-SW; however, Box 2 has few events with WNW-ESE trending sinistral and mostly NW-SE trending thrust nodal planes. In Box 3, most of the nodal planes show high-angle and low-angle E-W normal faulting, and a conjugate ENE-WSW and WNW-ESE in strike-slip motion.

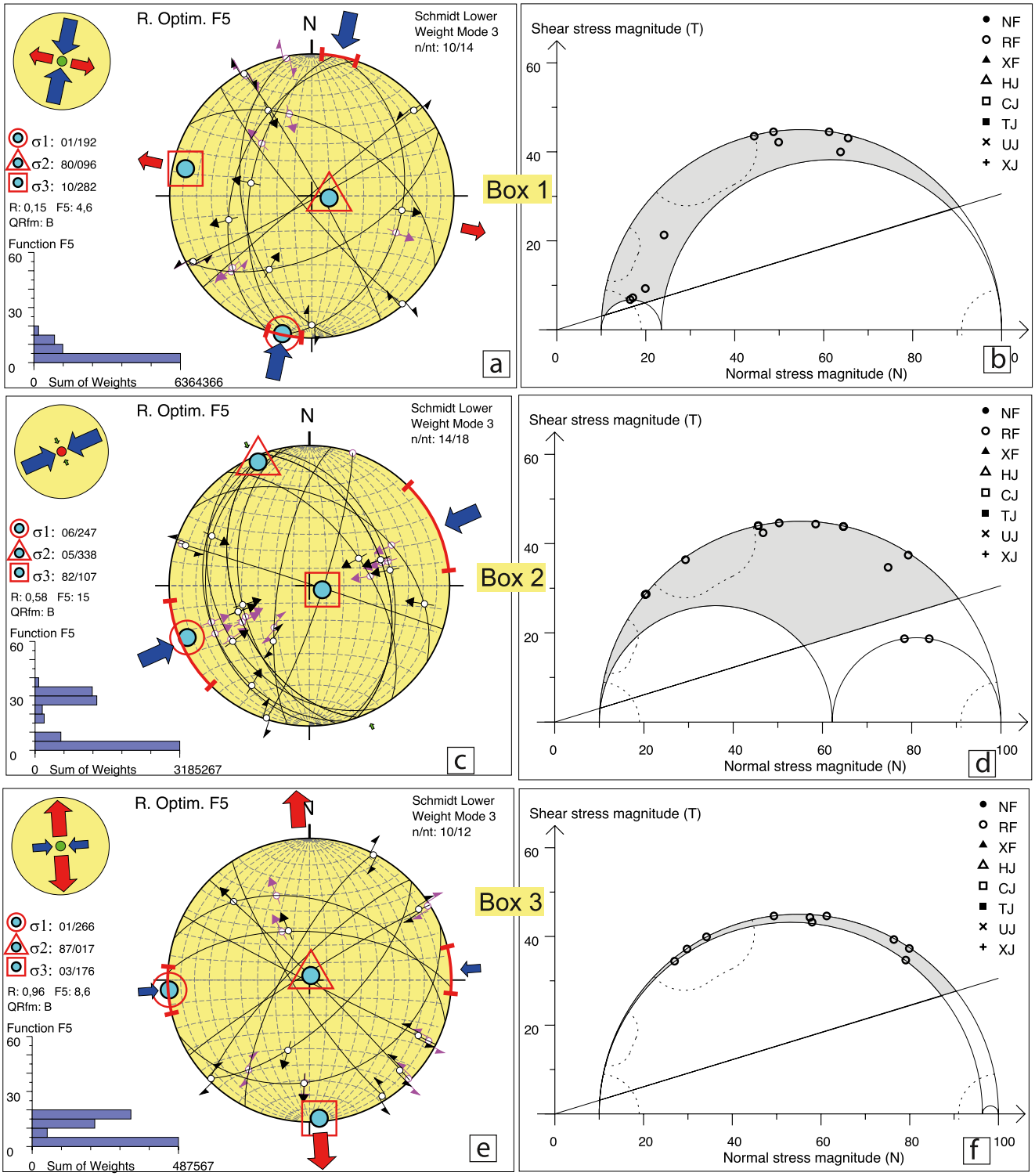

Figure 7. Results of stress tensors from the inversion of earthquake focal mechanism solutions along (a and b) offshore Gulf of Guinea and onshore western Africa continental margin and (c–e) interior of the Congo Craton (Congo Basin and Kasai Block), represented by sub-regional boxes (see Figures 2b and 3). Left: stereonet, lower hemisphere, with focal planes as great circles and the slip lines as arrows (outward-pointing arrows: normal faulting, inward-pointing arrows: thrust faulting, double arrows: strike-slip faulting). Stress symbols as in Delvaux et al. (1997). Histogram of misfit values. Frohlich triangles (Frohlich, 1992) displaying the type of individual focal mechanism (black dot) and the stress regime of the resulting stress tensor (colored large dot). Left: Mohr diagrams corresponding to the solution obtained, with dimensionless magnitudes, and the line of initial friction sloping at $\varphi = 20°$.

Table 1
Stress Parameters Associated With the Focal Mechanism Solution of Earthquakes in Box 1 (Gulf of Guinea and Continental Margin), Box 2 (Congo Basin), and Box 3 (Kasai Block) in Figure 2b

			$\sigma 1$		$\sigma 2$		$\sigma 3$							
	n	*nt*	*Pl*	*Az*	*Pl*	*Az*	*Pl*	*Az*	Reg	QRfm	*R*	*R′*	Stress regime	SHmax
Box 1	10	14	1	192	80	96	10	282	SS	B	0.15	1.85 ± 0.17	Compressional strike-slip	12 ± 7.1
Box 2	14	18	6	247	5	338	82	107	TF	B	0.58	2.58 ± 0.44	Pure compression	66 ± 19.6
Box 3	10	12	1	266	87	28	2	175	SS	B	0.96	1.04 ± 0.25	Extensional strike-slip	86 ± 9.6

Note. n: number of data used, *nt*: total data, *Pl* and *Az*: plunge and azimuth of principal compressive stress tensors, *R′*: index regime; Reg: Regime, QRfm: Quality rank of focal mechanism.

4.4. Slip Tendency of Preexisting Fault Systems

The application of stress tensors to the fault systems mapped onshore along the coastal margin and the continental interior (Box 1–3 sub-region) shows that several faults that are more likely to be reactivated. When applying box 1 stress regime, most of the NW-SE, NNE to NE-SW orientated subvertical strike-slip faults and few NW-SE trending law-angle thrust faults in all the four field systems (ISF, SFS, WCF1, WCFS2) can be reactivated (Figures 8a, 8g, 9a, and 9g). Particularly for ISF, SFS and WCFS2, most of strike slip faults showed the highest values of TsN = 80%–100%. Here, the WNW- to E-W -oriented faults show the lowest values of TsN, suggesting they could not be reactivated in such stress field. The WNW- to E-W planes are mis-oriented for reactivation as they plot beneath the failure envelope (residual strength envelope) in the Mohr diagram (blue circles in Figures 8d, 8f, 8j, 8k, 9d, 9f, 9j, and 9k). Overall, using a slope friction angle of 30°, most of the faults are in position of higher reactivation as indicated by the Mohr diagram (Figures 8d, 8j, 9d, and 9j).

In Box 2 stress field, N-S to NNE-SW trending faults of IFS, SFS, WCFS2 have very low shear stress and high normal resolved stress in the Mohr diagram, and have low TsN values. This suggest that they have a low sliding potential and are unlikely to be reactivated in this stress field. Furthermore, the Application of Box 2 is only able to reactivate the WCFS1 that is mainly dominated by NW-SE thrust fault that show very high slip tendency. All strike-slip fault are impossible to be reactivated in this stress field.

Under the stress regime of box 3, the situation of possible favorable planes to be reactivated is relatively similar as for the application of the tensor of box 1. The main difference is the sense of movement on the faults which is the opposite in the two tests. Also, Box 1 stress tensor favor slip on NNE-SSW and NNW-SSE subvertical faults while Box 3 stress tensor favor slip on ENE-WSW and ESE-WNW subvertical faults. Except for the WCFS1 (Figure 9b) that cannot be reactivated in Box 3 stress field, the IFS, SFS, and WCFS2 show that the WNW-ESS and ENE-WSW trending strike-slip faults (Figures 8c, 8i, 9c, and 9i) are the most likely to be reactivated with high TsN values (>60%).

5. Discussion

5.1. The Stress Regime of Earthquakes Along the Western Africa Continental Margin

The regional clustering of earthquakes along and in the vicinity of preexisting tectonic lineaments (Figures 3a and 4) and the stress tests performed in this study (Figures 7–9) show that earthquakes along the continental margin of western Africa and western Central Africa are likely associated with seismogenic reactivation of preexisting fault systems inherited from past tectonic events. As we only have one field site (e.g., SF, see Figure 3b) that was in the vicinity of the earthquakes data and the other (IFS, WCFS1, WCFS2) in a zone that have not yet recorded seismic event. Therefore, all of three stress tensors of the boxes were assessed if it was the one that was reactivating the existing fault network. These structures consist primarily of brittle shear zones developed during the Eburnean orogeny (Proterozoic), Pan-African Orogeny (Proterozoic), and the opening of the Central and South Atlantic (Late Cretaceous). The results of stress inversion and stress application in this study show that most of the actual fault planes would be NW-SW, NNW-SSE, WNW-ESW, N-S, NNE to NE-SW, ENE-WSW and less likely E-W trending strike-slip faults/normal faults or NW-SE and E-W trending thrust-faults in Box 1, Box 2 and Box 3 sub-regions. These faults orientations match most of the fracture systems described in the area

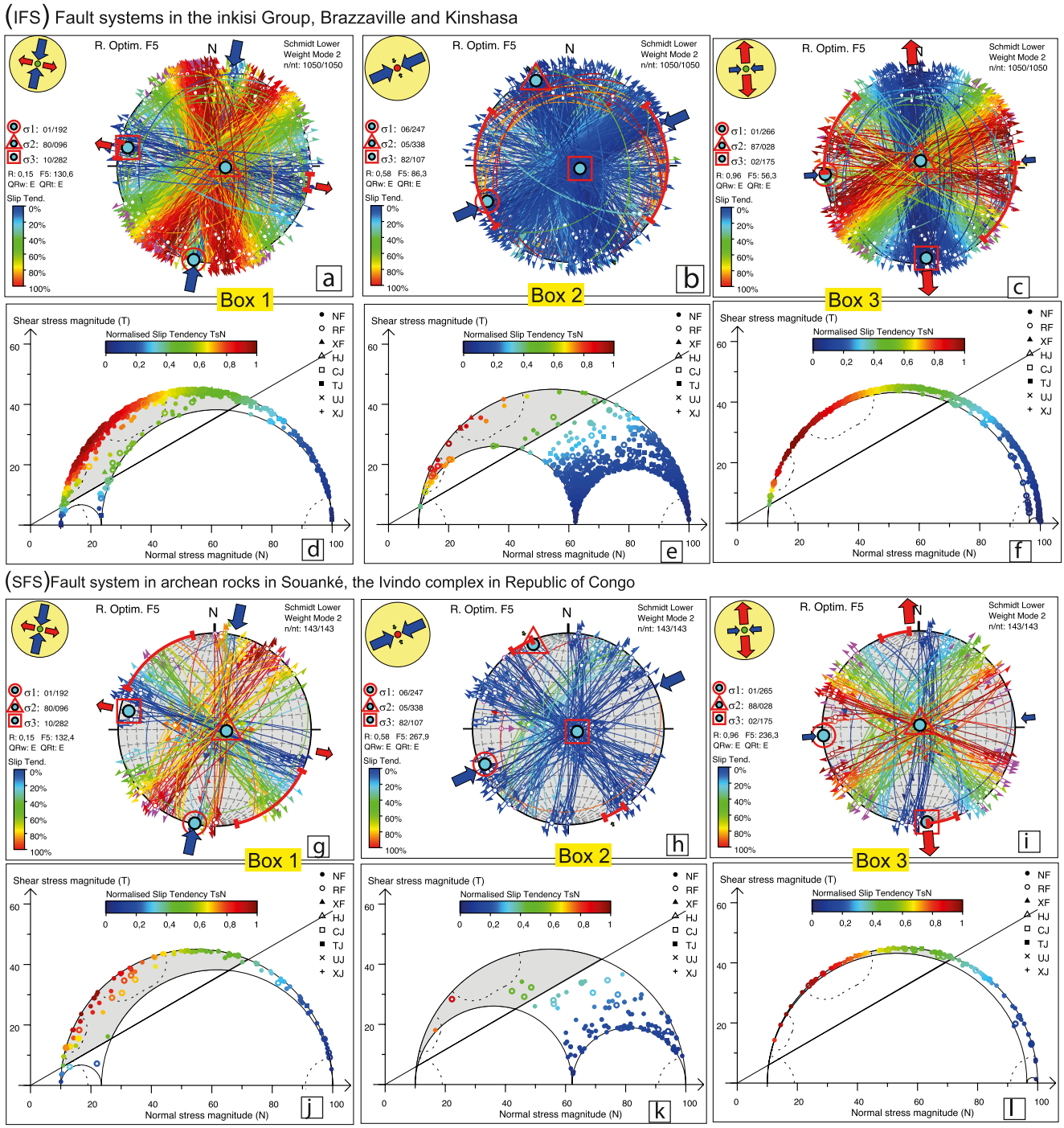

Figure 8. The application of the stress inversion results for Box 1 (left column), Box 2 (right column) and Box 3 on IFS and SFS fault systems and the resulting Slip Tendency values associated with their Mohr-Coulomb stress states. The slip tendency estimate associated with each fault segment is presented as color-coded planes in both the stereoplots and their adjoining Mohr diagrams.

(SFS, IFS, WCFS1, WCFS2) and in the literature (Figures 8 and 9). In Box 1 and Box 2 sub-regions, the NW- and E-W -oriented thrust faults probably correspond to the orientation of structures within the West-Congo Belt and thrust sheets of the Oubanguides Belt respectively. Both the strike-slip faults and normal faults deform every unit in the sub-regions from Archean through the Cretaceous units. Also, based on the visited field sites with seismic events, the earthquake epicenters are generally located in the vicinity of the large strike-slip fault systems or normal fault zones. For Box 1 (Figure 7), strike-slip faults, normal and reverse faults would likely corre-

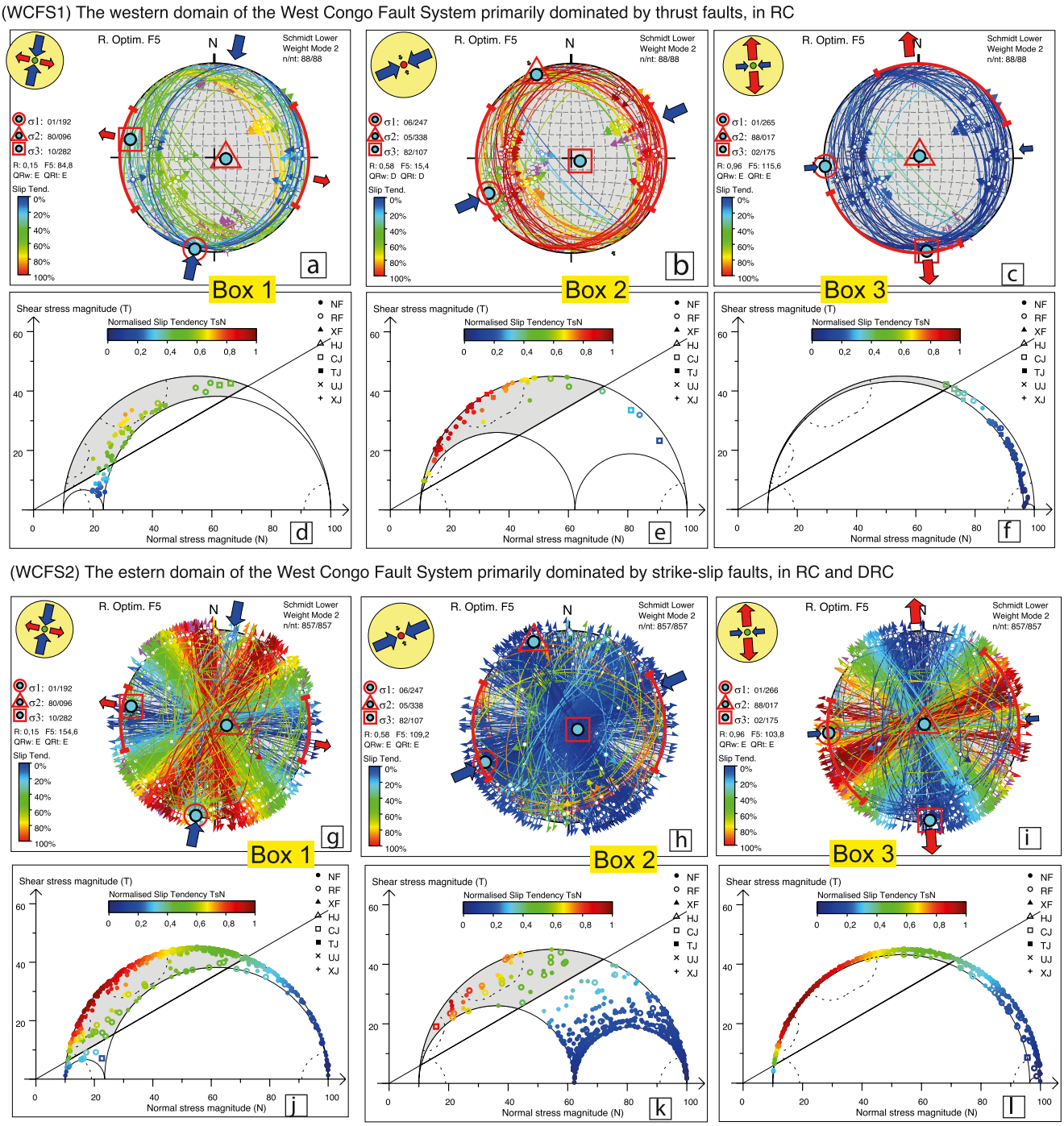

Figure 9. The application of the stress inversion results for Box 1 (left column), Box 2 (right column) and Box 3 on WCFS1 and WCFS2 fault systems and the resulting Slip Tendency values associated with the Mohr-Coulomb stress states. The slip tendency estimate associated with each fault segment is presented as color-coded planes in both the stereoplots and their adjoining Mohr diagrams.

spond to N-S and NNE-trending strike-slip and thrust fault systems of the Dahomeyide Belt (Affaton et al., 1991; Villeneuve & Cornée, 1994) which were later reactivated either in normal faulting or strike-slip faulting. This is the same case for observation in SFS (Figure 5f) and IFS.

The orientations of nodal planes used in stress inversion determination are consistent with the kinematics of some of the strike-slip, normal, and thrust fault systems with high values of slip tendency in Box 1, Box 2 and Box 3

stress fields applied to these faults systems in the area (Figures 7–9). The NNW-SSE and NNE-SSW features would play as dextral strike-slip faults and sinistral strike-slip faults under the stress regime in Box 1. This situation is satisfied in perfectly in the SFS fault system of Souanké (Figure 8g), in WCFS2 and with some faults in IFS (Figure 8a). For instance, in the coastal margin, the Monatélé earthquake in Cameroon was associated with a NE-SW trending strike-slip sinistral fault (Ngatchou et al., 2018). This clearly supports the kinematics of actual faults plan acting in this coastal margin. From the coastal margin to inland continent, the results show that there is a partition in stress regime within the western central African continental plate. On the coastal margin a strike-slip faulting regime with a minor compressional regime component prevails, while inland, the regime is more compressive with a moderate strike-slip faulting component. This transition of regime explains why NW-SE to NNE-SE strike-slip faults/normal faults show the highest tendency to be reactivated in the costal margin areas during the past or present-day. While for the continental interior areas, the most probable reactivated structures are NW-thrust faults/normal faults systems and less likely strike-slip faults. Delvaux et al. (2017) proposed the development of strike-slip deformation of the Inkisi Group during the opening of the south Atlantic and suggested that the event was associated with the last phase of continental break-up with sub-horizontal maximum compressive stress that is oriented N-S. The inferred stress field of the break-up phase is similar to the stress field calculated for Box 1 stress-field in this study (Figure 7a). This would indicate that Box 1 stress field was once acting on the cratonic interior sub-regions but is now restricted to the continental margin areas.

Overall, several studies have speculated that preexisting fractures are hosting earthquakes along the continental margins and interior of western Africa but lack details of the ambient stress field and the evidence for coseismic surface fault rupture or presence of active fault scarps (Amponsah, 2002; Ayele, 2002; Blundell, 1976; Bouka Biona & Founga, 2001; Kutu, 2013; Olugboji et al., 2021; Sykes, 1978). Here, with our stress analysis, we provide insight into the control of contemporary stress regimes on the occurrence of intraplate earthquakes in the region.

5.2. The Inherited Weakness of the Preexisting Fault Systems

Our stress analysis shows that the structural geometries of preexisting fault zone fracture surfaces make them favorably oriented for reactivation in the contemporary stress field. However, although fault orientation and their coefficient of friction in the Mohr-Coulomb space may determine whether a preexisting fault can reactivate, they do not determine whether faults would reactivate by stable creep or by seismic rupture. The susceptibility of faults to seismic or stable creep reactivation is determined by the frictional stability of the faulted rocks at the contemporary temperature and pressure conditions at depth in the crust (Blanpied et al., 1998; Dieterich, 1979; Ikari et al., 2011; Marone, 1998). This phenomenon is true for both active plate boundary settings (e.g., Carpenter et al., 2009) and intraplate settings (e.g., Kolawole et al., 2019).

Our field observations of the basement- and sedimentary-hosted fault systems show widespread occurrence of gouge and hydrothermal mineralization along the fault zones (Figures 6a–6f). These include calcite veins, quartz veins, palygorskite gouge fill, a mix of palygorskite and calcite, and iron stains (i.e., Mees et al., 2019). The presence of calcite and quartz veining suggests that there were intense fluid circulation along the fault zones in the past; and the occurrence and the occurrence of sheared calcite mineralization along the fault surfaces as evidenced by slip fibers and chatter marks (Figures 6a–6c) suggest that several of these faults have been experienced shear reactivation after the episode of hydrothermal mineralization. Further, the subvertical geometry of the mineralized large strike-slip fault systems implies that they must extend deeply into the crust. This is supported by the widespread presence of calcite mineralization along fault zones in both the crystalline basement rocks of the West Congo Belt and the IFS overlying Inkisi Sandstone units which suggest that the large strike-slip fault systems in the sedimentary cover are likely rooted directly into the basement and both structural levels have shared at least one episode of hydrothermal circulation in the past. More importantly, the most-common host minerals along the fault zones, calcite and palygorskite, are known from laboratory experiments to show frictional instability ($0 > a-b > -0.013$) at temperature and pressure conditions relevant to a seismogenic depth interval in the upper crust (Kolawole et al., 2019; Sánchez-Roa et al., 2017; Verberne et al., 2015). Thus, potentially presenting an additional control on earthquake nucleation along the fault systems that are favorably oriented to the present-day stress field (Figures 7a–7f).

Although there is no record of earthquake occurrence yet in the locations of our field observations, since the areas represent the southern continuation of the same terranes and fault systems of areas of recorded seismicity in the north, we think the field observations are relevant for the northern areas. Overall, the fault zones investigated in the field appear to be generally dry in present-day, indicating that the fault zone mineralization are likely associated with paleo-hydrothermal circulation episodes Asides from the Cameroon Volcanic Line and the Angolan Bié Dome, hot springs are very rare along the continental margin and there is no large-scale geothermal high-anomaly along the western Africa onshore continental margin areas (Macgregor, 2020; Waring et al., 1965). The occurrence of hot springs in both the Cameroon Volcanic Line and Bié Dome are understandable since both are known zones of localized mantle upwelling (Reusch et al., 2010; Walker et al., 2016). Further, we suggest that the sparseness of hot springs in the region suggests that seismic reactivation of the intraplate fault zones is not likely driven by crustal circulation of hot fluids. Therefore, considering the widespread occurrence of minerals like calcite, quartz, and palygorskite along the fault zones, we suggest that the seismic stability conditions of the faulted rocks at depth may be contributing to the susceptibility of the onshore fault zones to seismic reactivation.

5.3. Possible Origins of Stress Loading Along the Western Africa Continental Margin

Aside from the Cameroon Volcanic Line and Bié Dome in Angola, where active mantle processes are driving magmatic activities and associated earthquakes (De Plaen et al., 2014; Tabod et al., 1992; Ubangoh et al., 1997), the origin of stress loading leading to seismogenic rupture of preexisting faults in the onshore areas of the western Africa's continental margin remains controversial and poorly understood (Olugboji et al., 2021). The proposed mechanisms include variations of lithospheric structure and gravitational potential energy associated with mid-oceanic ridge (Mahatsente & Coblentz, 2015; Medvedev, 2016), the reactivation of local basement fractures by far-field tectonic stresses from mantle processes along the Cameroon volcanic line, post-rift crustal relaxation along the rifted margin, landward continuation of oceanic fracture zones, and induced earthquakes triggered by groundwater extraction (Olugboji et al., 2021).

Regional observations of basement deformation onshore along the western Africa coastal margins show the presence of fault and fracture systems that trend parallel or sub-parallel to the oceanic fracture zones but are not extend offshore to link with the oceanic fracture zones. The zone of earthquake clustering along the Ghana coastal margin, shown in Figures 2a and 3a is collocated with the southern projections of NNE-trending Quaternary faults (Akwapim, Lokossa, and Séhoué Faults) which appear to splay northwards from the northeastern tip zone of the Chain Fracture Zone offshore, suggested to exhibit a Reidel horsetail-pattern geometry within the fracture zone (Burke, 1969). However, Burke (1969) rightfully noted that there is no evidence of continuity of fault trace further inland from this region. Further east of the Ghana region, brittle deformation of exhumed granitic massifs and gnessic terranes further inland in SW Nigeria show the pervasive presence of satellite-scale ENE-trending fracture systems (Anifowose & Kolawole, 2012) which trend parallel to the near-shore segments of the oceanic fracture zones (see oceanic fracture zone rose diagram in Figure 2a). Likewise, in this study, onshore large-scale lineament mapping and detailed field mapping of fault systems show the presence of ENE-to-NE-trending fault systems that do not extend directly offshore, but also trend parallel to the near-shore segments of the oceanic fracture zones (Figures 1, 2a, and 3a). It was also proposed that channeling of melt along the northeastward extension of the Ascension Fracture Zone across the continent-ocean boundary and further onshore influenced the development of the Cameroon Volcanic Line (Reusch et al., 2010). However, the NE-SW oriented extensional structures would have formed parallel to the shortening axis and approximately to the maximum compressive stress (Woodcock & Schubert, 1994).

In addition to the observation of similar structural trends between oceanic fracture zones and onshore fault and fracture systems, our analysis shows that the stresses acting on the offshore oceanic fracture zones are comparable with the stresses acting along the onshore areas of the continental margin (Figures 7a, 7b and 7e); and that the onshore fault systems have a high slip tendency in this contemporary stress field (Figures 8 and 9). Some of the oceanic fracture zones are active, thus representing intraplate faults that are possibly activated by far-field strain transfer from transform faults along the spreading ridges (Figure 2a; Meghraoui et al., 2019). Based on the results of stress analysis in this study, we propose that zones of higher stress magnitudes along distal offshore oceanic fracture zones extend further into the continent and may be driving stress loading on pre-stressed, favorably oriented fault systems onshore, along the continental margin.

6. Conclusions

In this study, we compute the contemporary stress field along the coastal margin of western Africa and some of the interior cratonic areas, map pre-existing fault systems in basement and sedimentary outcrops along the margin, and assess the reactivation potential of the mapped structural planes. Our results show that:

- Intraplate earthquakes along the continental margin of West Africa and western Central Africa cluster along or in the vicinity of preexisting basements-rooted faults, suggesting a potential for brittle reactivation of preexisting structures.
- Stress regimes switch from a transpressive stress regime (NNE-SSW -oriented maximum horizontal compressive stress, SHmax) offshore and near the coastal margins, compressive stress regime (NE-SW -oriented SHmax) in the Congo Basin, to transtensive stress regime (E-W -oriented SHmax) in the Kasai Block of the Congo Craton.
- In this contemporary stress field, the pre-existing NNE-, NNW-, and N-S -trending strike-slip faults and normal faults show a high slip tendency (60%–100%), suggesting a high likelihood to be reactivated. Whereas in the cratonic interior of western Central Africa, the NW- and N-S -trending thrust faults are the most probable structures to be reactivated.
- In both the basement and sedimentary cover rocks, paleo-hydrothermal alterations of the fault zones are common. Although, in present-day, the fault zones are generally dry, the high likelihood of reactivation (based on our stress tests) and presence of fault rock frictionally unstable materials on fault planes (minerals like palygorskite and calcite) suggest that the faults may be susceptible to frictional instability and earthquake nucleation during their reactivation.
- Our stress analysis show that the regional stresses acting on offshore oceanic fracture zones are compatible with the stresses acting along the onshore areas of the continental margin; and that the onshore pre-existing strike-slip faults, which are parallel to the oceanic fracture zones, have a high slip tendency in this contemporary stress field.

We propose that zones of higher stress magnitudes along distal offshore oceanic fracture zones extend further into the continent and may be driving stress loading on pre-stressed, favorably oriented fault systems onshore, along the continental margin.

Conflict of Interest

The authors declare no conflicts of interest relevant to this study.

Data Availability Statement

The earthquake data used in this study can be downloaded in the International Seismic Center (ISC) (http://www.isc.ac.uk/), the United States Geological Survey (USGS) (https://www.usgs.gov/programs/earthquake-hazards/earthquakes), the Global Centroid-Moment-Tensor (CMT) (https://www.globalcmt.org/), and the GFZ GEOFON earthquake catalogs (https://geofon.gfz-potsdam.de/eqinfo/list.php). The focal mechanism data and field measurements that support the analysis in this study are provided in the supplementary documents of the manuscript. The data can be retrieved in the following repository https://doi.org/10.7910/DVN/B6QARK. The version 5.9.1 of the Win-Tensor free-access software was used to determine stress from focal mechanism and for the assessment of fault slip tendency. The software can be downloaded from http://damiendelvaux.be/Tensor/tensor-index.html (Delvaux, 2012).

Acknowledgments
This work is part of the PhD thesis of Nkodia Hardy. It is funded by Coopération Belge and ACCORDCAD, under the GEORES4DEV program, for his PhD through the support of the Royal Museum of Central Africa. We thank the reviewers and particularly Mustapha Meghraoui, Joao Fonseca, Chris Morley for their great help to improve this manuscript. We also thank Mr. Elvis Kongota and Prof. Valentin Kanda Nkula for their administrative help in DRC.

References

Adepelumi, A. A., Ako, B. D., Ajayi, T. R., Olorunfemi, A. O., Awoyemi, M. O., & Falebita, D. E. (2008). Integrated geophysical mapping of the Ifewara transcurrent fault system, Nigeria. *Journal of African Earth Sciences*, *52*(4), 161–166. https://doi.org/10.1016/j.jafrearsci.2008.07.002

Affaton, P., Rahaman, M. A., Trompette, R., & Sougy, J. (1991). The Dahomeyide Orogen: Tectonothermal evolution and relationships with the Volta Basin. In *The West African orogens and circum-Atlantic correlatives* (pp. 107–122). Springer.

Ajakaiye, D., Hall, D., Millar, T., Verheijen, P., Awad, M., & Ojo, S. (1986). Aeromagnetic anomalies and tectonic trends in and around the Benue Trough, Nigeria. *Nature*, *319*(6054), 582–584. https://doi.org/10.1038/319582a0

Akame, J. M., Owona, S., Hublet, G., & Debaille, V. (2020). Archean tectonics in the sangmelima granite-greenstone terrains, Ntem Complex (NW Congo craton), southern Cameroon. *Journal of African Earth Sciences*, *168*, 103872. https://doi.org/10.1016/j.jafrearsci.2020.103872

Akame, J. M., Schulz, B., Owona, S., & Debaille, V. (2021). Monazite EPMA-CHIME dating of Sangmelima granulite and granitoid rocks in the Ntem Complex, Cameroon: Implications for Archean tectono-thermal evolution of NW Congo craton. *Journal of African Earth Sciences*, *181*, 104268. https://doi.org/10.1016/j.jafrearsci.2021.104268

Alvarez, P., & Maurin, J.-C. (1991). Evolution sédimentaire et tectonique du bassin protdrozoïque supérieur de Comba (Congo): Stratigraphie séquentielle du Supergroupe Ouest-Congolien et modèle d'amortissement sur décrochements dans le contexte de la tectogènèse panafricaine. *Precambrian Research*, *50*(1–2), 137–171. https://doi.org/10.1016/0301-9268(91)90051-b

Ambraseys, N. N., & Adams, R. D. (1986). Seismicity of West Africa. *Seismicity of West Africa*, *4*(6), 679–702.

Amponsah, P. E. (2002). Seismic activity in relation to fault systems in southern Ghana. *Journal of African Earth Sciences*, *35*(2), 227–234. https://doi.org/10.1016/S0899-5362(02)00100-8

Amponsah, P., Leydecker, G., & Muff, R. (2012). Earthquake catalogue of Ghana for the time period 1615–2003 with special reference to the tectono-structural evolution of south-east Ghana. *Journal of African Earth Sciences*, *75*, 1–13. https://doi.org/10.1016/j.jafrearsci.2012.07.002

Angelier, J. (1975). Sur l'analyse de mesures recueillies dans des sites faillés: L'utilité d'une confrontation entre les méthodes dynamiques et cinématiques: Erratum. *Comptes Rendus de l'Académie des Sciences*, *283*, 466.

Angelier, J. (1989). From orientation to magnitudes in paleostress determinations using fault slip data. *Journal of Structural Geology*, *11*(1/2), 37–50. https://doi.org/10.1016/0191-8141(89)90034-5

Angelier, J., & Mechler, P. (1977). Sur une methode graphique de recherche des contraintes principales egalement utilisables en tectonique et en seismologie: La methode des diedres droits. *Bulletin de la Societe Geologique de France*, *7*(6), 1309–1318. https://doi.org/10.2113/gssgfbull.S7-XIX.6.1309

Anifowose, A. Y. B., & Kolawole, F. (2012). Emplacement tectonics of Idanre Batholith, West Africa. *Comunicação Geológicas*, *99*(2).

Antobreh, A. A., Faleide, J. I., Tsikalas, F., & Planke, S. (2009). Rift–shear architecture and tectonic development of the Ghana margin deduced from multichannel seismic reflection and potential field data. *Marine and Petroleum Geology*, *26*(3), 345–368. https://doi.org/10.1016/j.marpetgeo.2008.04.005

Assumpção, M. (1998). Seismicity and stresses in the Brazilian passive margin. *Bulletin of the Seismological Society of America*, *88*(1), 160–169.

Awoyemi, M. O., Hammed, O. S., Falade, S. C., Arogundade, A. B., Ajama, O. D., Iwalehin, P. O., & Olurin, O. T. (2017). Geophysical investigation of the possible extension of Ifewara fault zone beyond Ilesa area, southwestern Nigeria. *Arabian Journal of Geosciences*, *10*(2), 27. https://doi.org/10.1007/s12517-016-2813-z

Awoyemi, M., & Onyedim, G. (2004). Relationship between air photo lineament and fracture patterns of Ilesha, southwestern Nigeria. *African Geoscience Review*, *11*(1), 81–90.

Ayele, A. (2002). Active compressional tectonics in central Africa and implications for plate tectonic models: Evidence from fault mechanism studies of the 1998 earthquakes in the Congo basin. *Journal of African Earth Sciences*, *35*(1), 45–50. https://doi.org/10.1016/s0899-5362(02)00098-2

Barth, A., Wenzel, F., & Giardini, D. (2007). Frequency sensitive moment tensor inversion for light to moderate magnitude earthquakes in eastern Africa. *Geophysical Research Letters*, *34*(15), L15302. https://doi.org/10.1029/2007GL030359

Batumike, M. J., Kampunzu, A. B., & Cailteux, J. H. (2006). Petrology and geochemistry of the Neoproterozoic Nguba and Kundelungu Groups, Katangan Supergroup, southeast Congo: Implications for provenance, paleoweathering and geotectonic setting. *Journal of African Earth Sciences*, *44*(1), 97–115. https://doi.org/10.1016/j.jafrearsci.2005.11.007

Benkhelil, J. (1989). The origin and evolution of the Cretaceous Benue Trough (Nigeria). *Journal of African Earth Sciences (and the Middle East)*, *8*(2–4), 251–282. https://doi.org/10.1016/s0899-5362(89)80028-4

Blanpied, M. L., Tullis, T. E., & Weeks, J. D. (1998). Effects of slip, slip rate, and shear heating on the friction of granite. *Journal of Geophysical Research*, *103*(B1), 489–511. https://doi.org/10.1029/97JB02480

Blundell, D. J. (1976). Active faults in West Africa. *Earth and Planetary Science Letters*, *31*(2), 287–290. https://doi.org/10.1016/0012-821X(76)90221-1

Boudzoumou, F., & Trompette, R. (1988). La chaine panafricaine ouest-congolienne au Congo (Afrique equatoriale); un socle polycyclique charrie sur un domaine subautochtone forme par l'aulacogene du Mayombe et le bassin de l'Ouest-Congo. *Bulletin de la Societe Geologique de France*, *4*(6), 889–896. https://doi.org/10.2113/gssgfbull.iv.6.889

Bouenitela, T. T. V. (2019). *Le domaine paleoproterozoique (eburneen) de la chaine du Mayombe (Congo-Brazzaville): Origine et évolution tectono-métamorphique*. Université de Rennes 1.

Bouka Biona, C., & Sounga, J.-D. (2001). Corrélation entre la localisation des foyers des séismes et les zones de délimination des horsts et des grabens su soubassement de la Cuvette Congolaise (Afrique Centrale). *Annales Université Brazzaville*, *2*(1), 125–139.

Burbank, D. W., & Anderson, R. S. (2011). *Tectonic geomorphology*. John Wiley & Sons.

Burke, K. (1969). Seismic areas of the Guinea coast where Atlantic fracture zones reach Africa. *Nature*, *222*(5194), 655–657. https://doi.org/10.1038/222655b0

Calais, E., Camelbeeck, T., Stein, S., Liu, M., & Craig, T. J. (2016). A new paradigm for large earthquakes in stable continental plate interiors. *Geophysical Research Letters*, *43*(20), 10621–10637. https://doi.org/10.1002/2016GL070815

Carpenter, B. M., Marone, C., & Saffer, D. M. (2009). Frictional behavior of materials in the 3D SAFOD volume. *Geophysical Research Letters*, *36*(5), L05302. https://doi.org/10.1029/2008GL036660

Craig, T. J., Jackson, J. A., Priestley, K., & McKenzie, D. (2011). Earthquake distribution patterns in Africa: Their relationship to variations in lithospheric and geological structure, and their rheological implications. *Geophysical Journal International*, *185*(1), 403–434. https://doi.org/10.1111/j.1365-246X.2011.04950.x

De Carvalho, H., Tassinari, C., Alves, P. H., Guimarães, F., & Simões, M. C. (2000). Geochronological review of the Precambrian in western Angola: Links with Brazil. *Journal of African Earth Sciences*, *31*(2), 383–402. https://doi.org/10.1016/S0899-5362(00)00095-6

De Long, S. E., Dewey, J. F., & Fox, P. J. (1977). Displacement history of oceanic fracture zones. *Geology*, *5*(4), 199–202. https://doi.org/10.1130/0091-7613(1977)5<199:dhoofz>2.0.co;2

De Plaen, R. S. M., Bastow, I. D., Chambers, E. L., Keir, D., Gallacher, R. J., & Keane, J. (2014). The development of magmatism along the Cameroon Volcanic Line: Evidence from seismicity and seismic anisotropy. *Journal of Geophysical Research: Solid Earth*, *119*(5), 4233–4252. https://doi.org/10.1002/2013JB010583

de Wit, M. J., & Linol, B. (2015). Precambrian basement of the Congo Basin and its flanking terrains. In M. J. de Wit, F. Guillocheau, & M. C. J. de Wit (Eds.), *Geology and resource potential of the Congo Basin* (pp. 19–37). Springer. https://doi.org/10.1007/978-3-642-29482-2_2

Delteil, J.-R., Valery, P., Montadert, L., Fondeur, C., Patriat, P., & Mascle, J. (1974). Continental margin in the northern part of the Gulf of Guinea. In C. A. Burk & C. L. Drake (Eds.), *The geology of continental margins* (pp. 297–311). Springer. https://doi.org/10.1007/978-3-662-01141-6_22

Delvaux, D. (2011). Version 3.0 and above of the Win-Tensor Program. Retrieved from http://users.skynet.be/damien.delvaux/Tensor/tensor-index.html

Delvaux, D. (2012). Release of program Win-Tensor 4.0 for tectonic stress inversion: Statistical expression of stress parameters. In *Geophysical research abstracts* (Vol. 14). EGU General Assembly Vienna.

Delvaux, D., & Barth, A. (2010). African stress pattern from formal inversion of focal mechanism data. *Tectonophysics*, *482*(1), 105–128. https://doi.org/10.1016/j.tecto.2009.05.009

Delvaux, D., & Sperner, B. (2003). New aspects of tectonic stress inversion with reference to the TENSOR program. *Geological Society, London, Special Publications*, *212*(1), 75–100. https://doi.org/10.1144/gsl.sp.2003.212.01.06

Delvaux, D., Everaerts, M., Kongota Isasi, E., & Ganza Bamulezi, G. (2016). Intraplate compressional deformation in West-Congo and the Congo basin: Related to ridge-puch from the South Atlantic spreading ridge? In *EGU General Assembly Conference Abstracts* (Vol. *18*).

Delvaux, D., Ganza, G., Kongota, E., Fukiabantu, G., Mbokola, D., Boudzoumou, F., et al. (2017). The "fault of the Pool" along the Congo River between Kinshasa and Brazzaville, R (D) Congo is no more a myth: Paleostress from small-scale brittle structures. In *EGU General Assembly Conference Abstracts* (Vol. *19*, p. 15143).

Delvaux, D., Maddaloni, F., Tesauro, M., & Braitenberg, C. (2021). The Congo Basin: Stratigraphy and subsurface structure defined by regional seismic reflection, refraction and well data. *Global and Planetary Change*, *198*, 103407. https://doi.org/10.1016/j.gloplacha.2020.103407

Delvaux, D., Moeys, R., Stapel, G., Petit, C., Levi, K., Miroshnichenko, A., et al. (1997). Paleostress reconstructions and geodynamics of the Baikal region, central Asia, Part 2. Cenozoic rifting. *Tectonophysics*, *282*(1–4), 1–38. https://doi.org/10.1016/s0040-1951(97)00210-2

Dieterich, J. H. (1979). Modeling of rock friction: 1. Experimental results and constitutive equations. *Journal of Geophysical Research*, *84*(B5), 2161–2168. https://doi.org/10.1029/JB084iB05p02161

Fail, J. P., Montadert, L., Delteil, J. R., Valery, P., Patriat, P., & Schlich, R. (1970). Prolongation des zones de fractures de l'ocean Atlantique dans le golfe de Guinee. *Earth and Planetary Science Letters*, *7*(5), 413–419. https://doi.org/10.1016/0012-821X(70)90083-X

Fairhead, J. D., Green, C. M., Masterton, S. M., & Guiraud, R. (2013). The role that plate tectonics, inferred stress changes and stratigraphic unconformities have on the evolution of the West and Central African Rift System and the Atlantic continental margins. *Tectonophysics*, *594*, 118–127. https://doi.org/10.1016/j.tecto.2013.03.021

Fossen, H. (2016). *Structural geology*. Cambridge University Press.

Frohlich, C. (1992). Triangle diagrams: Ternary graphs to display similarity and diversity of earthquake focal mechanisms. *Physics of the Earth and Planetary Interiors*, *75*(1), 193–198. https://doi.org/10.1016/0031-9201(92)90130-N

Fullgraf, T., Callec, Y., Thiéblemont, D., Gloaguen, E., Charles, N., Métour, J., et al. (2015). *Notice explicative de la carte géologique de la République du Congo à 1/200 000, Feuille Dolisie. (F)*. Editions BRGM.

Gatsé Ebotehouna, C., Xie, Y., Adomako-Ansah, K., & Qu, Y. (2021). Petrology, geochemistry, and zircon U–Pb-Lu–Hf isotopes of granitoids from the Ivindo Basement Complex of the Souanké Area, Republic of Congo: Insights into the evolution of Archean continental crust. *Geological Journal*, *56*(9), 4861–4887. https://doi.org/10.1002/gj.4219

GEBCO Bathymetric Compilation Group 2021. (2021). *The GEBCO_2021 grid - A continuous terrain model of the global oceans and land*. NERC EDS British Oceanographic Data Centre NOC. https://doi.org/10.5285/c6612cbe-50b3-0cff-e053-6c86abc09f8f

Gerya, T. (2012). Origin and models of oceanic transform faults. *Tectonophysics*, *522–523*, 34–54. https://doi.org/10.1016/j.tecto.2011.07.006

Gorini, M. A., & Bryan, G. (1976). The tectonic fabric of the equatorial Atlantic and adjoining continental margins: Gulf of Guinea to the north-eastern Brazil. In *Paper presented at the Anais da Academia Brasileira de Ciências, Sao Paulo* (Vol. *48*, pp. 101–119).

Grigoli, F., Cesca, S., Priolo, E., Rinaldi, A. P., Clinton, J. F., Stabile, T. A., et al. (2017). Current challenges in monitoring, discrimination, and management of induced seismicity related to underground industrial activities: A European perspective. *Reviews of Geophysics*, *55*(2), 310–340. https://doi.org/10.1002/2016rg000542

Guiraud, M., Buta-Neto, A., & Quesne, D. (2010). Segmentation and differential post-rift uplift at the Angola margin as recorded by the transform-rifted Benguela and oblique-to-orthogonal-rifted Kwanza basins. *Marine and Petroleum Geology*, *27*(5), 1040–1068. https://doi.org/10.1016/j.marpetgeo.2010.01.017

Gupta, H. K., Rastogi, B. K., Mohan, I., Rao, C. V. R. K., Sarma, S. V. S., & Rao, R. U. M. (1998). An investigation into the Latur earthquake of September 29, 1993 in southern India. *Tectonophysics*, *287*(1), 299–318. https://doi.org/10.1016/S0040-1951(98)80075-9

Heezen, B. C., Bunce, E. T., Hersey, J. B., & Tharp, M. (1964). Chain and Romanche fracture zones. *Deep Sea Research and Oceanographic Abstracts*, *11*(1), 11–33. https://doi.org/10.1016/0011-7471(64)91079-4

Heezen, B. C., Tharp, M., Blackett, P. M. S., Bullard, E., & Runcorn, S. K. (1965). Tectonic fabric of the Atlantic and Indian Oceans and continental drift. *Philosophical Transactions of the Royal Society of London - Series A: Mathematical and Physical Sciences*, *258*(1088), 90–106. https://doi.org/10.1098/rsta.1965.0024

Heidbach, O., Rajabi, M., Cui, X., Fuchs, K., Müller, B., Reinecker, J., et al. (2018). The World Stress Map database release 2016: Crustal stress pattern across scales. *Tectonophysics*, *744*, 484–498. https://doi.org/10.1016/j.tecto.2018.07.007

Hensen, C., Duarte, J. C., Vannucchi, P., Mazzini, A., Lever, M. A., Terrinha, P., et al. (2019). Marine transform faults and fracture zones: A joint perspective integrating seismicity, fluid flow and life. *Frontiers of Earth Science*, *7*, 39. https://doi.org/10.3389/feart.2019.00039

Holford, S. P., Hillis, R. R., Hand, M., & Sandiford, M. (2011). Thermal weakening localizes intraplate deformation along the southern Australian continental margin. *Earth and Planetary Science Letters*, *305*(1), 207–214. https://doi.org/10.1016/j.epsl.2011.02.056

Hossié, G. (1980). *Contribution à l'étude structurale de la chaîne Ouest-congolienne(Pan-Africaine) dans le Mayombe congolais* (Thesis). University of Montpellier.

Ikari, M. J., Marone, C., & Saffer, D. M. (2011). On the relation between fault strength and frictional stability. *Geology*, *39*(1), 83–86. https://doi.org/10.1130/G31416.1

Jelsma, H. A., McCourt, S., Perritt, S. H., & Armstrong, R. A. (2018). The geology and evolution of the Angolan shield, Congo craton. In S. Siegesmund, M. A. S. Basei, P. Oyhantçabal, & S. Oriolo (Eds.), *Geology of Southwest Gondwana* (pp. 217–239). Springer International Publishing. https://doi.org/10.1007/978-3-319-68920-3_9

Junner, N. R., & Bates, D. A. (1941). *The Accra earthquake of 22nd June, 1939*. FJ Miller.

Kadima, E., Delvaux, D., Sebagenzi, S. N., Tack, L., & Kabeya, S. M. (2011). Structure and geological history of the Congo Basin: An integrated interpretation of gravity, magnetic and reflection seismic data. *Basin Research*, *23*(5), 499–527. https://doi.org/10.1111/j.1365-2117.2011.00500.x

Kadiri, A. U., & Kijko, A. (2021). Seismicity and seismic hazard assessment in West Africa. *Journal of African Earth Sciences*, *183*, 104305. https://doi.org/10.1016/j.jafrearsci.2021.104305

Keranen, K. M., & Weingarten, M. (2018). Induced seismicity. *Annual Review of Earth and Planetary Sciences*, *46*(1), 149–174. https://doi.org/10.1146/annurev-earth-082517-010054

Kessi, C. (1992). *Le socle Archéen et les formations ferrifères du Chaillu au Congo* (Thèse Doctorat). Université de Rennes 1.

Kolawole, F., Atekwana, E. A., Malloy, S., Stamps, D. S., Grandin, R., Abdelsalam, M. G., et al. (2017). Aeromagnetic, gravity, and Differential Interferometric Synthetic Aperture Radar analyses reveal the causative fault of the 3 April 2017 M_w 6.5 Moiyabana, Botswana, earthquake. *Geophysical Research Letters*, *44*(17), 8837–8846. https://doi.org/10.1002/2017gl074620

Kolawole, F., Johnston, C. S., Morgan, C. B., Chang, J. C., Marfurt, K. J., Lockner, D. A., et al. (2019). The susceptibility of Oklahoma's basement to seismic reactivation. *Nature Geoscience*, *12*(10), 839–844. https://doi.org/10.1038/s41561-019-0440-5

Krenkel, E. (1923). Die Seismizität Afrikas. *Zentralblatt für Mineralogie, Geologie und Palaontologie*, *6*, 173–183.

Kutu, J. M. (2013). Seismic and tectonic correspondence of major earthquake regions in southern Ghana with Mid-Atlantic transform-fracture zones. *International Journal of Geosciences*, *4*(10), 1326–1332. https://doi.org/10.4236/ijg.2013.410128

Lay, T. (2019). Chapter 4 - Reactivation of oceanic fracture zones in large intraplate earthquakes? In J. C. Duarte (Ed.), *Transform plate boundaries and fracture zones* (pp. 89–104). Elsevier. https://doi.org/10.1016/B978-0-12-812064-4.00004-9

Levandowski, W., Zellman, M., & Briggs, R. (2017). Gravitational body forces focus North American intraplate earthquakes. *Nature Communications*, *8*(1), 1–9. https://doi.org/10.1038/ncomms14314

Loemba, A. P. A., Nkodia, H. M. D.-V., Bazebizonza Tchiguina, N. C., Miyouna, T., & Boudzoumou, F. (2022). Tectonic and structural evolution of major shear zone in the Ntem-Chaillu Block, in the Ivindo region. In *Republic of Congo*. *Paper presented at the Tectonic Studies Group 2022, online* (p. 53).

Lund Snee, J.-E., & Zoback, M. D. (2020). Multiscale variations of the crustal stress field throughout North America. *Nature Communications*, *11*(1), 1951. https://doi.org/10.1038/s41467-020-15841-5

Macgregor, D. S. (2020). Regional variations in geothermal gradient and heat flow across the African plate. *Journal of African Earth Sciences*, *171*, 103950. https://doi.org/10.1016/j.jafrearsci.2020.103950

Mahatsente, R., & Coblentz, D. (2015). Ridge-push force and the state of stress in the Nubia-Somalia plate system. *Lithosphere*, *7*(5), 503–510. https://doi.org/10.1130/L441.1

Marone, C. (1998). Laboratory-derived friction laws and their application to seismic faulting. *Annual Review of Earth and Planetary Sciences*, *26*(1), 643–696. https://doi.org/10.1146/annurev.earth.26.1.643

Mascle, J., & Sibuet, J.-C. (1974). New pole for early opening of South Atlantic. *Nature*, *252*(5483), 464–465. https://doi.org/10.1038/252464a0

Mbéri Kongo, M. T. G. (2018). *Tectonique de la série des plateaux Batékés dans la zone de Inoni et d'Ekoti ya MonSeigneur, République du Congo* (Master thesis). Marien Ngouabi. https://doi.org/10.13140/RG.2.2.14583.34729

McCaffrey, R. (2008). Global frequency of magnitude 9 earthquakes. *Geology*, *36*(3), 263–266. https://doi.org/10.1130/G24402A.1

Medvedev, S. (2016). Understanding lithospheric stresses: Systematic analysis of controlling mechanisms with applications to the African plate. *Geophysical Journal International*, *207*(1), 393–413. https://doi.org/10.1093/gji/ggw241

Mees, F., Adriaens, R., Delgado-Huertas, A., Delvaux, D., Lahogue, P., Mpiana, C., & Tack, L. (2019). Palygorskite-bearing fracture fills in the Kinshasa area, DR Congo – An exceptional mode of palygorskite vein development. *South African Journal of Geology*, *122*(2), 173–186. https://doi.org/10.25131/sajg.122.0013

Meghraoui, M., Amponsah, P., Ayadi, A., Ayele, A., Bekoa, A., Bensuleman, A., et al. (2016). The Seismotectonic map of Africa. *Episodes*, *39*(1), 9–18. https://doi.org/10.18814/epiiugs/2016/v39i1/89232

Meghraoui, M., Amponsah, P., Bernard, P., & Ateba, B. (2019). Active transform faults in the Gulf of Guinea: Insights from geophysical data and implications for seismic hazard assessment. *Canadian Journal of Earth Sciences*, *56*(12), 1398–1408. https://doi.org/10.1139/cjes-2018-0321

Milesi, J. P., Frizon de Lamotte, D., de Kock, G., & Toteu, F. (2010). Tectonic map of Africa (2nd ed.).

Miranda, T. S., Neves, S. P., Celstino, M.-A. L., & Roberts, N. M. W. (2020). Structural evolution of the Cruzeiro do Nordeste shear zone (NE Brazil): Brasiliano-Pan-African-ductile-to-brittle transition and Cretaceous brittle reactivation. *Journal of Structural Geology*, *141*, 1–17. https://doi.org/10.1016/j.jsg.2020.104203

Miyouna, T., Dieu-Veill Nkodia, H. M., Essouli, O. F., Dabo, M., Boudzoumou, F., & Delvaux, D. (2018). Strike-slip deformation in the Inkisi formation, Brazzaville, Republic of Congo. *Cogent Geoscience*, *4*(1), 1542762. https://doi.org/10.1080/23312041.2018.1542762

Morris, A., Ferrill, D. A., & Henderson, D. B. (1996). Slip-tendency analysis and fault reactivation. *Geology*, *24*(3), 275–278. https://doi.org/10.1130/0091-7613(1996)024<0275:staafr>2.3.co;2

Moulin, M., Aslanian, D., & Unternehr, P. (2010). A new starting point for the South and Equatorial Atlantic Ocean. *Earth-Science Reviews*, *98*(1–2), 1–37. https://doi.org/10.1016/j.earscirev.2009.08.001

Musson, R. M. W. (1992). The seismicity of West and Central Africa. In S. J. Freeth, C. O. Ofoegbu, & K. M. Onuoha (Eds.), *Natural hazards in West and Central Africa* (pp. 7–11). Vieweg+Teubner Verlag. https://doi.org/10.1007/978-3-663-05239-5_2

Ngako, V., Affaton, P., Nnange, J. M., & Njanko, T. (2003). Pan-African tectonic evolution in central and southern Cameroon: Transpression and transtension during sinistral shear movements. *Journal of African Earth Sciences*, *36*(3), 207–214. https://doi.org/10.1016/s0899-5362(03)00023-x

Ngako, V., Jegouzo, P., & Nzenti, J.-P. (1991). Le cisaillement Centre Camerounais. Rôle structural et géodynamique dans l'orogenèse panafricaine. *Le Cisaillement Centre Camerounais. Rôle Structural et Géodynamique Dans l'orogenèse Panafricaine*, *313*(4), 457–463.

Ngatchou, H. E., Nguiya, S., Owona Angue, M., Mouzong, P. M., & Tokam, A. P. (2018). *Source characterization and tectonic implications of the M4.6 Monatélé (Cameroon) earthquake of 19 March 2005*. Geological Society of South Africa.

Njonfang, E., Ngako, V., Moreau, C., Affaton, P., & Diot, H. (2008). Restraining bends in high temperature shear zones: The "Central Cameroon Shear zone", Central Africa. *Journal of African Earth Sciences*, *52*(1–2), 9–20. https://doi.org/10.1016/j.jafrearsci.2008.03.002

Nkodia, H. M. D.-V., Boudzoumou, F., Miyouna, T., Ibarra-Gnianga, A., & Delvaux, D. (2021). A progressive episode of deformation in the foreland of the West-Congo Belt: From folding to brittle shearing. In *Republic of Congo*. *Paper presented at the European Gesosciences Union, online* (p. 1).

Nkodia, H. M. D.-V., Miyouna, T., Delvaux, D., & Boudzoumou, F. (2020). Flower structures in sandstones of the Paleozoic Inkisi Group (Brazzaville, Republic of Congo): Evidence for two major strike-slip fault systems and geodynamic implications. *South African Journal of Geology*, *123*(4), 531–550. https://doi.org/10.25131/sajg.123.0038

Nwankwoala, H., & Orji, O. (2018). An overview of earthquakes and tremors in Nigeria: Occurrences, distributions and implications for monitoring. *International Journal of Geology and Earth Sciences*, *4*, 56. https://doi.org/10.32937/IJGES.4.4.2018.56-76

Ofoegbu, C. O. (1985). A review of the geology of the Benue Trough, Nigeria. *Journal of African Earth Sciences*, *3*(3), 283–291. https://doi.org/10.1016/0899-5362(85)90001-6

Oha, I. A., Okonkwo, I. A., & Dada, S. S. (2020). Wrench tectonism and intracontinental basin sedimentation: A case study of the Moku sub-basin, upper Benue Trough, Nigeria. *Journal of Geography and Geology*, *12*(1), 65–75. https://doi.org/10.5539/jgg.v12n1p65

Okal, E. A., & Stewart, L. M. (1982). Slow earthquakes along oceanic fracture zones: Evidence for asthenospheric flow away from hotspots? *Earth and Planetary Science Letters*, *57*(1), 75–87. https://doi.org/10.1016/0012-821X(82)90174-1

Oladejo, O. P., Adagunodo, T. A., Sunmonu, L. A., Adabanija, M. A., Enemuwe, C. A., & Isibor, P. O. (2020). Aeromagnetic mapping of fault architecture along Lagos–Ore axis, southwestern Nigeria. *Open Geosciences*, *12*(1), 376–389. https://doi.org/10.1515/geo-2020-0100

Olugboji, T. M., Shirzaei, M., Lu, Y., Adepelumi, A. A., & Kolawole, F. (2021). On the origin of orphan tremors and intraplate seismicity in western Africa. *Earth and Space Science Open Archive ESSOAr*.

Reusch, A. M., Nyblade, A. A., Wiens, D. A., Shore, P. J., Ateba, B., Tabod, C. T., & Nnange, J. M. (2010). Upper mantle structure beneath Cameroon from body wave tomography and the origin of the Cameroon Volcanic Line. *Geochemistry, Geophysics, Geosystems*, *11*(10), Q10W07. https://doi.org/10.1029/2010GC003200

Sbar, M. L., & Sykes, L. R. (1973). Contemporary compressive stress and seismicity in eastern North America: An example of intra-plate tectonics. *GSA Bulletin*, *84*(6), 1861–1882. https://doi.org/10.1130/0016-7606(1973)84<1861:ccsasi>2.0.co;2

Schulte, S. M., & Mooney, W. D. (2005). An updated global earthquake catalogue for stable continental regions: Reassessing the correlation with ancient rifts. *Geophysical Journal International*, *161*(3), 707–721. https://doi.org/10.1111/j.1365-246X.2005.02554.x

Stein, S., Cloetingh, S., Sleep, N. H., & Wortel, R. (1989). Passive margin earthquakes, stresses and rheology. In S. Gregersen & P. W. Basham (Eds.), *Earthquakes at North-Atlantic passive margins: Neotectonics and postglacial rebound* (pp. 231–259). Springer Netherlands. https://doi.org/10.1007/978-94-009-2311-9_14

Suleiman, A. S., Doser, D. I., & Yarwood, D. R. (1993). Source parameters of earthquakes along the coastal margin of West Africa and comparisons with earthquakes in other coastal margin settings. *Tectonophysics*, *222*(1), 79–91. https://doi.org/10.1016/0040-1951(93)90191-L

Sykes, L. R. (1978). Intraplate seismicity, reactivation of preexisting zones of weakness, alkaline magmatism, and other tectonism postdating continental fragmentation. *Reviews of Geophysics*, *16*(4), 621–688. https://doi.org/10.1029/RG016i004p00621

Sánchez-Roa, C., Faulkner, D. R., Boulton, C., Jimenez-Millan, J., & Nieto, F. (2017). How phyllosilicate mineral structure affects fault strength in Mg-rich fault systems. *Geophysical Research Letters*, *44*(11), 5457–5467. https://doi.org/10.1002/2017GL073055

Tabod, C. T., Fairhead, J. D., Stuart, G. W., Ateba, B., & Ntepe, N. (1992). Seismicity of the Cameroon volcanic line, 1982–1990. *Tectonophysics*, *212*(3), 303–320. https://doi.org/10.1016/0040-1951(92)90297-J

Talwani, P. (Ed.). (2014). *Intraplate Earthquakes*. https://doi.org/10.1017/cbo9781139628921

Tchameni, R., Mezger, K., Nsifa, N. E., & Pouclet, A. (2000). Neoarchæan crustal evolution in the Congo Craton: Evidence from K rich granitoids of the Ntem Complex, southern Cameroon. *Journal of African Earth Sciences*, *30*(1), 133–147. https://doi.org/10.1016/S0899-5362(00)00012-9

Thiéblemont, D., Castaing, C., Billa, M., Bouton, P., & Préat, A. (2009). Notice explicative de la carte géologique et des ressources minérales de la République Gabonaise à 1/1000000. *Programme Sysmin*, *8*, 384.

Turnbull, R. E., Allibone, A. H., Matheys, F., Fanning, C. M., Kasereka, E., Kabete, J., et al. (2021). Geology and geochronology of the Archean plutonic rocks in the northeast Democratic Republic of Congo. *Precambrian Research*, *358*, 106133. in–press. https://doi.org/10.1016/j.precamres.2021.106133

Tuttle, M. P., Schweig, E. S., Sims, J. D., Lafferty, R. H., Wolf, L. W., & Haynes, M. L. (2002). The earthquake potential of the New Madrid seismic zone. *Bulletin of the Seismological Society of America*, *92*(6), 2080–2089. https://doi.org/10.1785/0120010227

Ubangoh, R. U., Ateba, B., Ayonghe, S. N., & Ekodeck, G. E. (1997). Earthquake swarms of Mt Cameroon, West Africa. *Journal of African Earth Sciences*, *24*(4), 413–424. https://doi.org/10.1016/S0899-5362(97)00072-9

Verberne, B. A., Niemeijer, A. R., De Bresser, J. H. P., & Spiers, C. J. (2015). Mechanical behavior and microstructure of simulated calcite fault gouge sheared at 20–600°C: Implications for natural faults in limestones. *Journal of Geophysical Research: Solid Earth*, *120*(12), 8169–8196. https://doi.org/10.1002/2015JB012292

Villeneuve, M., & Cornée, J. J. (1994). Structure, evolution and palaeogeography of the West African craton and bordering belts during the Neoproterozoic. *Precambrian Research*, *69*(1), 307–326. https://doi.org/10.1016/0301-9268(94)90094-9

Walker, R. T., Telfer, M., Kahle, R. L., Dee, M. W., Kahle, B., Schwenninger, J.-L., et al. (2016). Rapid mantle-driven uplift along the Angolan margin in the late Quaternary. *Nature Geoscience*, *9*(12), 909–914. https://doi.org/10.1038/ngeo2835

Waring, G. A., Blankenship, R. R., & Bentall, R. (1965). *Thermal springs of the United States and other countries: A summary*. U.S. Government Printing Office.

Wiens, D. A., & Stein, S. (1983). Age dependence of oceanic intraplate seismicity and implications for lithospheric evolution. *Journal of Geophysical Research*, *88*(B8), 6455–6468. https://doi.org/10.1029/jb088ib08p06455

Wiens, D. A., & Stein, S. (1985). Implications of oceanic intraplate seismicity for plate stresses, driving forces and rheology. *Tectonophysics*, *116*(1–2), 143–162. https://doi.org/10.1016/0040-1951(85)90227-6

Wilson, J. T. (1965). A new class of faults and their bearing on continental drift. *Nature*, *207*(4995), 343–347. https://doi.org/10.1038/207343a0

Woodcock, N. H., & Schubert, C. (1994). Continental strike-slip tectonics. *Continental Deformation*, 251–263.

Zoback, M. L. (1992). Stress field constraints on intraplate seismicity in eastern North America. *Journal of Geophysical Research*, *97*(B8), 11761–11782. https://doi.org/10.1029/92JB00221

Zoback, M. L., & Richardson, R. M. (1996). Stress perturbation associated with the Amazonas and other ancient continental rifts. *Journal of Geophysical Research*, *101*(B3), 5459–5475. https://doi.org/10.1029/95JB03256

Erratum

In the original publication of this article the affiliation for Folarin Kolawole was incorrectly listed as "Department of Geology, Royal Museum for Central Africa, Tervuren, Belgium." The correct affiliation is "Lamont-Doherty Earth Observatory, Columbia University, New York, NY, USA." The affiliation was corrected after first online publication, and this updated version may be considered the version of record.